Journal of Medicinal Chemistry

Article

pubs.acs.org/jmc

Discovery of Highly Selective and Orally Active Lysophosphatidic Acid Receptor-1 Antagonists with Potent Activity on Human Lung Fibroblasts

Yimin Qian,*[,†] Matthew Hamilton,[†] Achyutharao Sidduri,[†] Stephen Gabriel,[†] Yonglin Ren,[‡] Ruoqi Peng,[‡] Rama Kondru,[†] Arjun Narayanan,[†] Terry Truitt,[§] Rachid Hamid,[§] Yun Chen,[§] Lin Zhang,[∥] Adrian J. Fretland,[⊥] Ruben Alvarez Sanchez,[⊥] Kung-Ching Chang,[‡] Matthew Lucas,[†] Ryan C. Schoenfeld,[†] Dramane Laine,[†] Maria E. Fuentes,[‡] Christopher S. Stevenson,[‡] and David C. Budd[‡]

[†]Discovery Chemistry, [‡]Discovery Inflammation and Respiratory Diseases, [§]Discovery Technology, [∥]Pharmaceutical and Analytical Research, and [⊥]Drug Metabolism and Pharmacokinetics, Small Molecule Research, Pharmaceutical Research and Early Drug Development, Hoffmann-La Roche, 340 Kingsland Street, Nutley, New Jersey 07110, United States

ABSTRACT: Lysophosphatidic acid is a class of bioactive phospholipid that mediates most of its biological effects through LPA receptors, of which six isoforms have been identified. The recent results from LPA1 knockout mice suggested that blocking LPA1 signaling could provide a potential novel approach for the treatment of idiopathic pulmonary fibrosis. Here, we report the design and synthesis of pyrazole- and triazole-derived carbamates as LPA1-selective and LPA1/3 dual antagonists. In particular, compound **2**, the most selective LPA1 antagonist reported, inhibited proliferation and contraction of normal human lung fibroblasts (NHLF) following LPA stimulation. Oral dosing of compound **2** to mice resulted in a dose-dependent reduction of plasma histamine levels in a murine LPA challenge model. Furthermore, we applied our novel antagonists as chemistry probes and investigated the contribution of LPA1/2/3 in mediating the pro-fibrotic responses. Our results suggest LPA1 as the major receptor subtype mediating LPA-induced proliferation and contraction of NHLF.

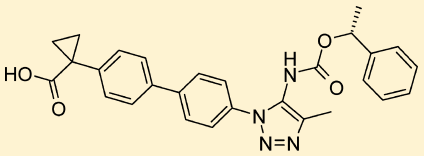

LPA1 IC_{50} = 25 nM, LPA3 IC_{50} >30 μM

INTRODUCTION

Idiopathic pulmonary fibrosis (IPF) represents the most severe form of interstitial pneumonias with a typical survival time of between three to five years after diagnosis. In addition, the lack of pharmaceutical treatments capable of altering the natural course of the disease underlies the exceptionally high unmet medical need and underscores the urgent necessity of identifying and developing novel efficacious treatment options. Although the exact molecular mechanisms of IPF are incompletely understood, it is recognized that the pathogenesis of pulmonary fibrosis is characterized by excessive extracellular matrix (ECM) protein deposition into lung alveolar interstitium leading to irreversible scarring, loss of function of the capillary alveolar unit, impaired gas exchange, and ultimately respiratory failure and death. Numerous pathways have been implicated in driving these diverse processes, highlighting the complexity of the pathophysiological mechanisms driving interstitial lung fibrosis.[1,2] The paucity of approved therapies that demonstrate robust efficacy for IPF is most likely due to the involvement of multiple pathways and mechanisms that ultimately contribute to irreversible lung scarring. The lung myofibroblast represents the central effector cell in pulmonary fibrosis by virtue of the ability of this cell type to synthesize and secrete extracellular matrix proteins.[2] Thus, pathways that act to induce the accumulation of interstitial lung myofibroblasts or promote their synthetic, profibrotic properties represent attractive pharmaceutical targets for the treatment of IPF.

Lysophosphatidic acid (LPA) is a class of biologically active phospholipids produced from lysophosphatidyl choline (LPC) catalyzed by the enzyme autotaxin.[3] LPA exerts a wide range of cellular responses, such as calcium mobilization, cell proliferation, cell transformation, and chemotaxis through a family of membrane bound GPCRs.[4] There are at least six LPA receptors (LPAR1−6) identified and characterized, with LPA1/2/3 from the EDG family sharing a relatively high homology.[5,6] LPA has been demonstrated to induce the proliferation of lung fibroblasts,[7] to promote the differentiation of lung fibroblasts to myofibroblasts,[8] and to augment fibroblast-mediated contraction of released three-dimensional collagen gels[9] underscoring the importance of this pathway in mediating profibrotic responses of lung fibroblasts *in vitro*. Using an *in vivo* murine unilateral ureteral obstruction (UUO) model to study renal fibrosis, expression of LPA1 was significantly up-regulated, while LPA3 was down-regulated, with no change in expression of LPA2 or LPA4 reported.[10] In the *in vivo* model of murine bleomycin-induced pulmonary fibrosis, LPA levels were increased in bronchoalveolar lavage fluid (BALF) following lung injury.[11] In support of a role of the LPA pathway in mediating lung fibrosis in response to bleomycin challenge, LPA1 knockout mice displayed a significant reduction in fibroblast recruitment, reduced vascular leakage, and increased

Received: July 13, 2012
Published: August 15, 2012

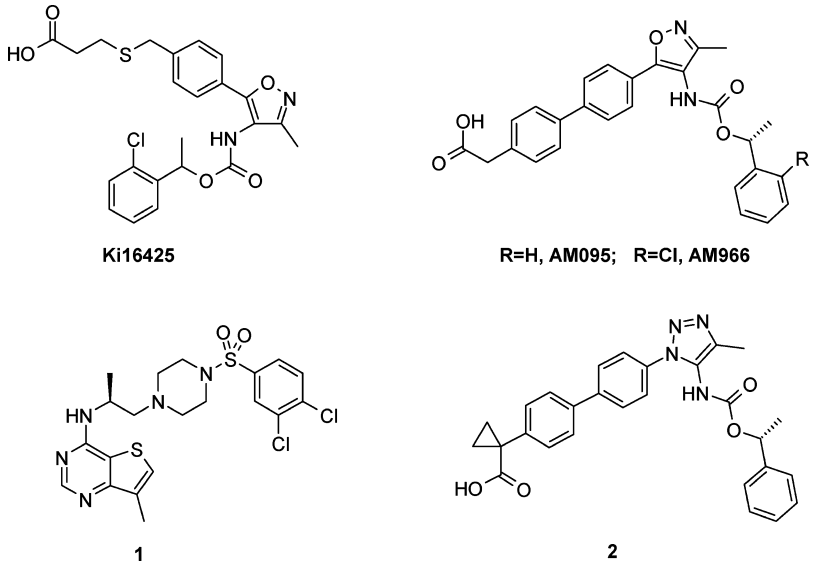

Figure 1. Structures of LPAR antagonists.

Scheme 1. Preparation of Compounds 3−10[a]

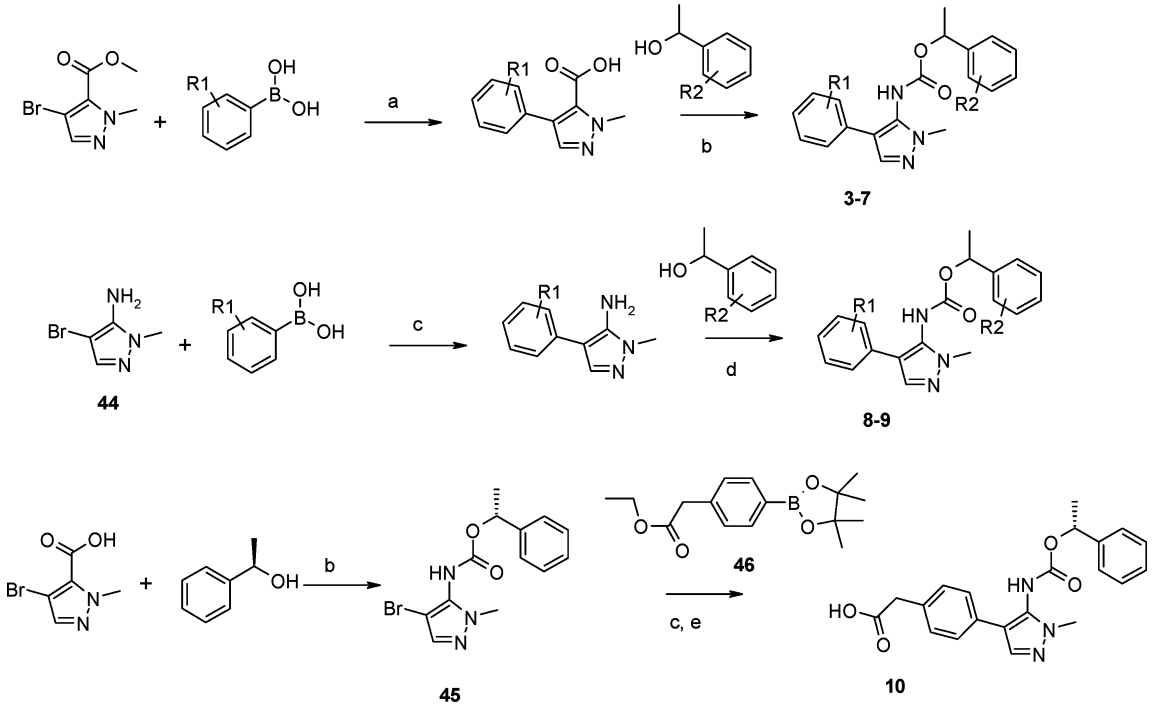

[a]Reaction conditions: (a) (i) $Pd(PPh_3)_4$ (cat), Cs_2CO_3, DMF, 80 °C; (ii) LiOH (aq), THF, 60 °C; (b) diphenylphosphoryl azide, triethylamine, toluene, 85 °C; (c) X-Phos (cat), $Pd(OAc)_2$ (cat), K_3PO_4, toluene/water, 95 °C; (d) triphosgene, triethylamine, dichloromethane, 85 °C; (e) THF/LiOH (aq), rt.

survival following bleomycin challenge compared to wild-type animals.[11] Additional murine models of pulmonary fibrosis such as the radiation-induced model of lung fibrosis report the possible involvement of LPA1 and LPA3 in driving the fibrotic responses.[12] In IPF patients, LPA levels were elevated in BALF, and LPA1 was identified as the predominant LPA receptor expressed in lung fibroblasts and was responsible for mediating enhanced migration of these cells.[11] Similarly, in our own studies we have also detected the expression of LPA1, LPA2, LPA3, LPA4, and LPA6 using quantitative PCR with the predominant isoform being LPA1 in normal human lung fibroblasts (NHLFs) and lung fibroblasts isolated from IPF patients (unpublished data). Taken together, this preclinical and clinical data suggests that targeting the LPA1 receptor could provide a novel therapeutic approach to treat IPF.

Several LPAR antagonists have been reported in the literature.[13−16] These antagonists have been classified as lipid-like molecules, such as nonhydrolyzable LPA analogues, and non lipid-like small molecules. The first non lipid-like LPAR antagonist, Ki16425, was reported as a dual LPA1/3 antagonist.[17] On the basis of the structure of Ki16425, biphenyl substituted isoxazole analogues AM095 and AM966 were

dx.doi.org/10.1021/jm301022v | J. Med. Chem. 2012, 55, 7920−7939

Scheme 2. Preparation of Compounds 11−20[a]

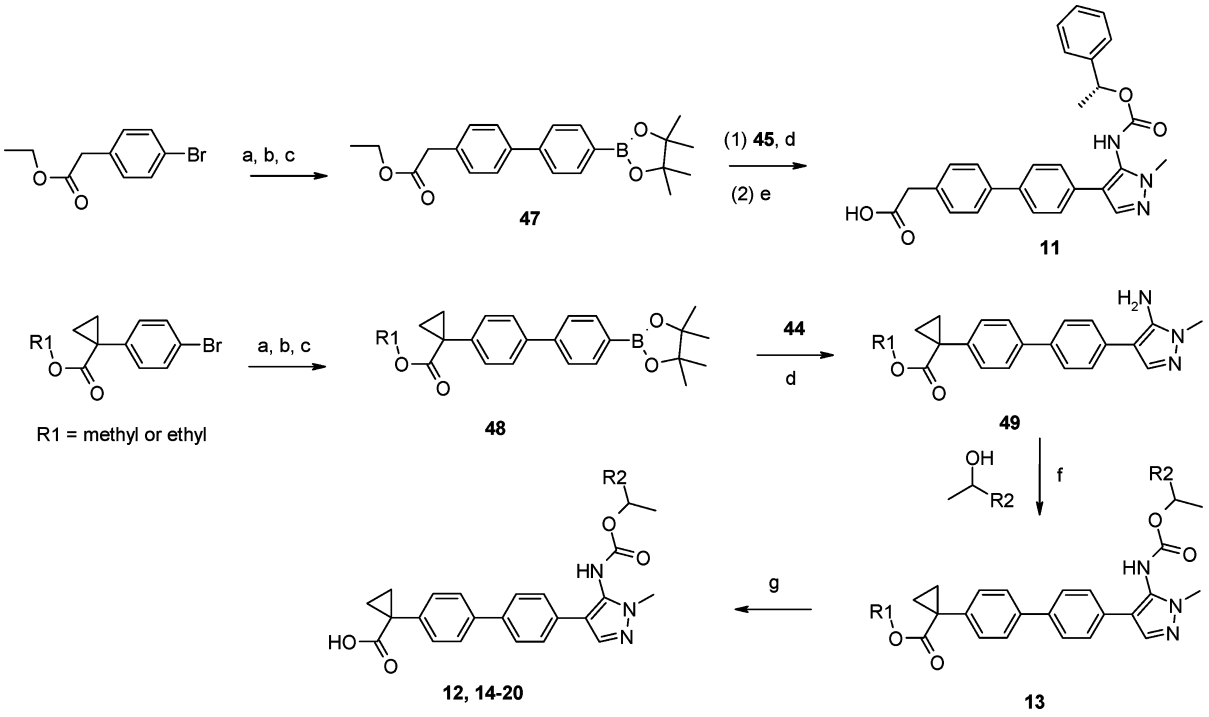

[a]Reaction conditions: (a) 4-hydroxyphenylboronic acid, $Pd(PPh_3)_4$ (cat), K_2CO_3, DMF; (b) $(CF_3SO_2)_2O$, triethylamine, dichloromethane, −78 °C to rt; (c) bis(pinacolato)diboron, KOAc, $PdCl_2$(dppf) (cat), dioxane, 90 °C; (d) X-Phos (cat), $Pd(OAc)_2$ (cat), K_3PO_4, toluene/water, 100 °C; (e) LiOH (aq), THF, rt; (f) triphosgene, triethylamine, dichloromethane, 85 °C; (g) NaOH (aq), ethanol, THF, rt.

reported as orally active, selective LPA1 antagonists.[18−20] Recently, LPA2 signaling has also been implicated in LPA-induced $\alpha v\beta 6$ integrin-mediated TGF-β activation.[21] LPA2-selective antagonists have also been reported (compound **1** in Figure 1).[22]

In order to identify novel LPA1-selective antagonists, we undertook a bioisostere approach and discovered pyrazole and triazole-derived carboxylic acids as LPA1-selective and LPA1/3 dual antagonists. In particular, compound **2** (Figure 1) to our knowledge represents the most selective LPA1 antagonist so far reported. Compound **2** demonstrated dose-dependent oral efficacy in blocking LPA-induced histamine release in mice. Furthermore, we applied our novel LPAR antagonists as chemical probes to study the contribution of LPAR isoforms in mediating the pro-fibrotic responses of normal human lung fibroblasts (NHLFs) in response to LPA stimulation. Our results clearly suggest LPA1, but not LPA2 or LPA3, is the major receptor mediating LPA-stimulated proliferation and contraction in NHLFs. Herein we report the design, synthesis, and biological studies of a novel series of LPA1 antagonists (compounds **2**−**43**) from the substituted pyrazole and triazole chemical class.

CHEMISTRY

Compounds **3**−**10** were prepared as described in Scheme 1. The commercially available 4-bromo-1-methyl-1*H*-pyrazole-5-carboxylic acid methyl ester was reacted with an arylboronic acid under Suzuki coupling conditions. Following saponification and Curtius rearrangement, compounds **3**−**7** were obtained. Alternatively, aminopyrazole **44** was reacted with an arylboronic acid under Suzuki coupling conditions. The resulting 5-amino-4-aryl-1-methylpyrazole was converted to the corresponding carbamate **8**−**9** through the intermediate isocyanate. For the preparation of compound **10**, 4-bromo-1-methypyrazole-5-carboxylic acid was first converted to carbamate **45**, which was further coupled with arylboronate **46** followed by saponification.

The preparation of compounds **11**−**20** is described in Scheme 2. The required biphenylboronic acid esters **47** and **48** were synthesized in three steps from the corresponding arylbromide. Compound **11** was obtained from the coupling of **47** with **45** followed by saponification. Using the same synthetic sequence, the cyclopropanecarboxylic acid analogues **12**−**20** were prepared as shown in Scheme 2.

The synthesis of *N*-aryltriazole analogues is described in Scheme 3. The reaction of arylazide with substituted alkyne gave triazole derivatives. The desired triazole was confirmed by NOE analysis. Following the sequence of saponification, Curtius rearrangement, biaryl coupling, and the final saponification, the acetic acid derivative (compound **21**), cyclopropanecarboxylic acid derivatives (**2**, **22**−**28**, **31**−**32**), and *N*-acylsulfonamide **29** were synthesized. The preparation of compound **30** was through the conversion of the intermediate cyanide to the corresponding tetrazole using methods previously described in the literature.[23]

Scheme 4 describes the synthesis of 4-*N*-aryl-3-amino-4*H*-[1,2,4]triazole analogue **33**. 4-Bromoaniline was converted to 2-methyl-1-arylisothiourea through a sequence of thioisocyanate formation, thiourea formation, and then methylation of the thiourea. After displacement of the methylthio group by hydrazine and subsequent ring formation with formic acid, 4-*N*-aryl-3-amino-4*H*-[1,2,4]triazole **52** was formed. Conversion of the arylbromide to the corresponding biphenyl derivative followed by carbamate formation and final saponification gave compound **33**.

dx.doi.org/10.1021/jm301022v | J. Med. Chem. 2012, 55, 7920−7939

Scheme 3. Synthesis of *N*-Aryltriazole Compounds 2 and 21−32[a]

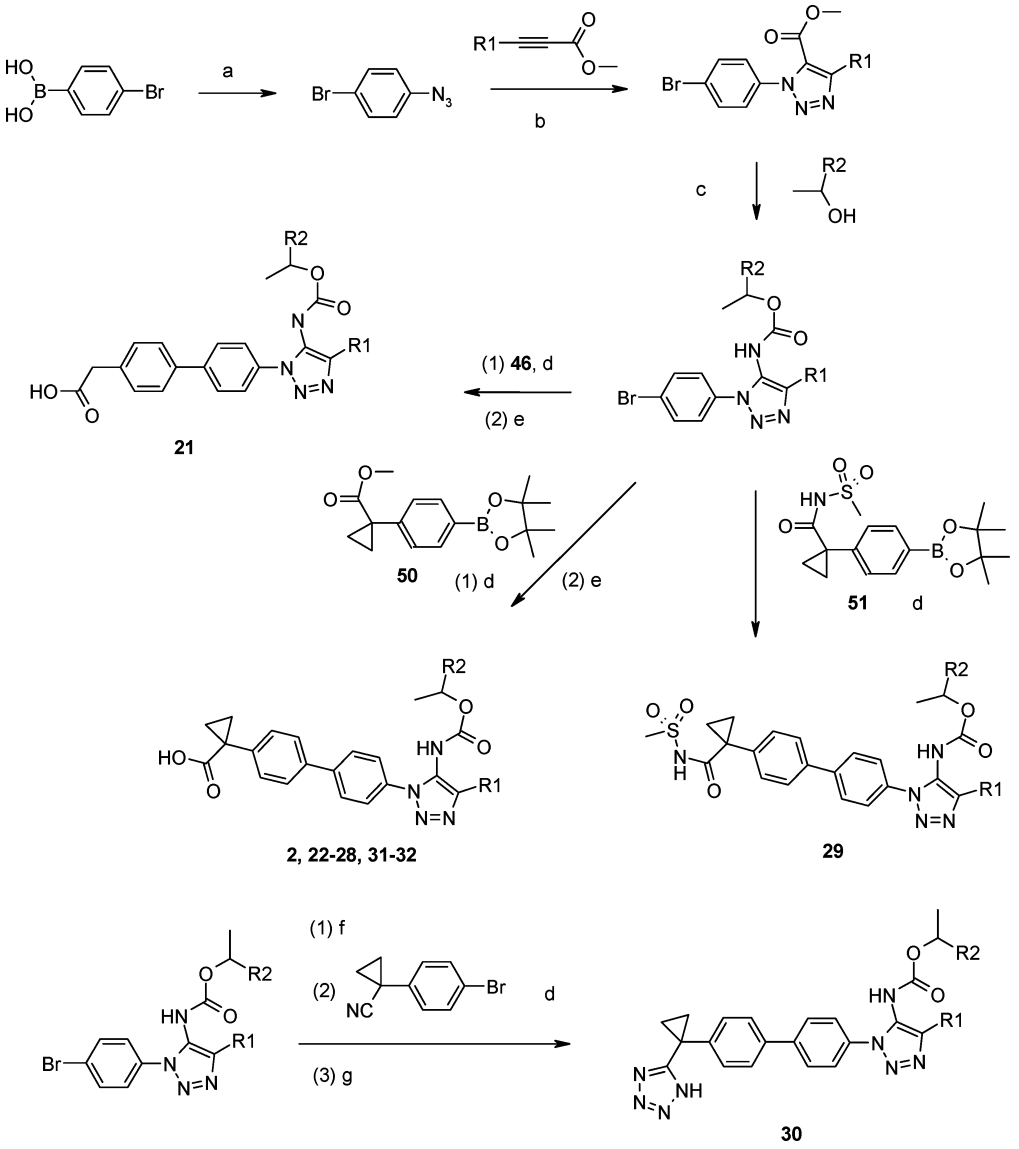

[a]Reaction conditions: (a) sodium azide, $Cu(OAc)_2$ (cat), methanol, rt; (b) toluene, sealed vessel, 150 °C, 4.5 h; (c) (i) LiOH (aq), THF, rt; (ii) diphenylphosphoryl azide, triethylamine, toluene, 65 °C; (d) S-Phos (cat), $Pd(OAc)_2$ (cat), K_3PO_4, toluene/water, 100 °C, 4 h; (e) NaOH (aq), THF, ethanol, rt; (f) bis(pinacolato)diboron, KOAc, $PdCl_2$(dppf) (cat), dioxane, 90 °C; (g) $TMSN_3$, n-Bu_2SnO (2 equiv), 100 °C, 15 h.

Finally, the synthesis of *N*-methyltriazole analogues **34**−**43** is described in Scheme 5. The required *N*-methyltriazole was formed through the reaction of an arylacetylene derivative with trimethylsilymethylazide. The structures of the two regioisomers were assigned by NOE analysis. Following the deprotection of the trimethylsilyl group and ester saponification, 1*N*-methyl-4-aryl-[1,2,3]-triazole-5-carboxylic acid and 1*N*-methyl-5-aryl-[1,2,3]-triazole-4-carboxylic acid were obtained. Conversion of the carboxylic acid to compounds **34**−**42** was carried out using the same method described in Scheme 3. For the preparation of the cyclohexane acetic acid analogue **43**, 4-iodocyclohexane acetic acid ethyl ester was coupled with an arylbromide through the formation of an alkyl zinc intermediate. The 1,4-substitutions of cyclohexane in **43** compose a mixture of cis/trans isomers.

RESULTS AND DISCUSSION

The design of novel bioisosteres has been practiced in drug discovery to optimize drug−target interactions.[24] We envisioned that aminopyrazole and aminotriazole could function as bioisosteres of the aminoisoxazole in Ki16425 and AM095. In particular, these novel heterocyclic bioisosteres could provide unique selectivity toward LPAR isoforms. To this end, we investigated the potential of *N*-methyl-5-aminopyrazole as a bioisostere of 4-amino-3-methylisoxazole. Compounds prepared in Scheme 1 were tested in a fluorometric imaging plate reader (FLIPR) assay using an engineered Chem-1 cell line overexpressing the human LPA1 or LPA3 receptors. The natural ligand LPA (18:1) was used to stimulate calcium mobilization at a final concentration of 1 μM. To prevent false positives in the FLIPR assay, compounds were also tested in wild-type Chem-1 cell lines without LPAR overexpression and stimulated with ionomycin. LPA1 and LPA3 antagonist activity is expressed as IC_{50}, the compound concentration to inhibit

dx.doi.org/10.1021/jm301022v | J. Med. Chem. 2012, 55, 7920−7939

Scheme 4. Synthesis of 4-*N*-Aryl-[1,2,4]triazole Derivative 33[a]

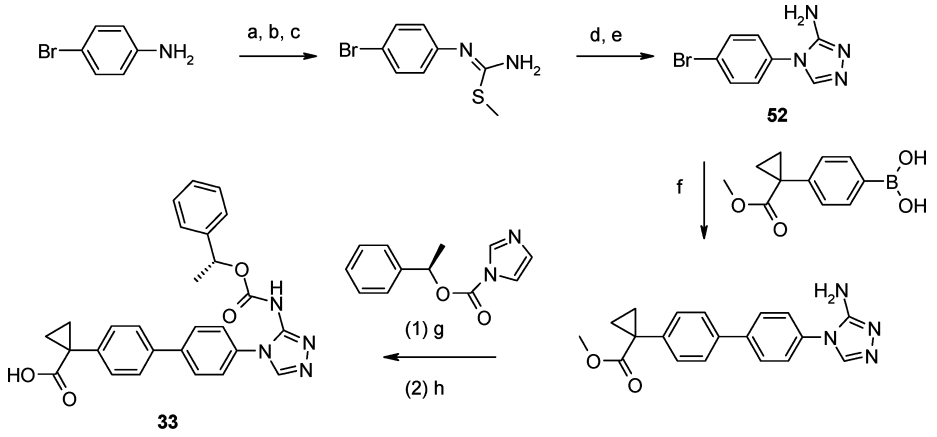

[a]Reaction conditions: (a) thiophosgene, $CaCO_3$, dichloromethane; (b) NH_3/THF; (c) MeI, methanol, rt; (d) hydrazine monohydrate; (e) formic acid, 120 °C, 3.5 h; (f) $PdCl_2$(dppf) (cat), Na_2CO_3 (aq), dioxane, 100 °C, 24 h; (g) LiHMDS, THF; (h) LiOH (aq), THF.

Scheme 5. Synthesis of Compounds 34−43[a]

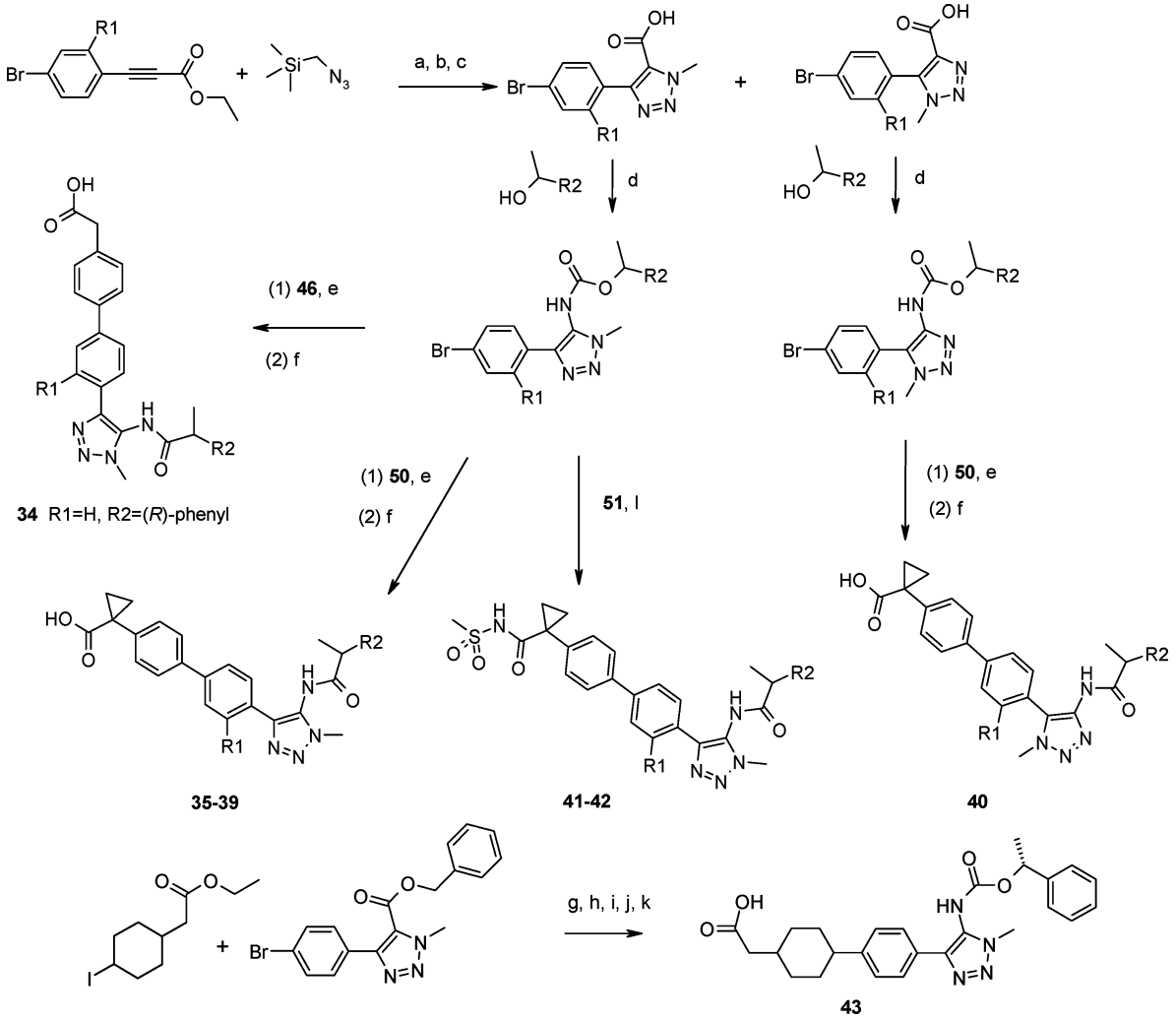

[a]Reaction conditions: (a) benzene, reflux, 4 h; (b) TBAF, THF, 0 °C; (c) LiOH (aq), THF, rt; (d) diphenylphosphoryl azide, triethylamine, toluene, 80 °C; (e) X-Phos (cat), $Pd(OAc)_2$ (cat), K_3PO_4, toluene/water, 100 °C; (f) NaOH (aq), THF, ethanol, rt; (g) activated zinc, THF; (h) $Pd(OAc)_2$ (cat), S-Phos (cat), THF; (i) Pd/C, H_2; (j) diphenylphosphoryl azide, (*R*)-phenylethanol, triethylamine, 80 °C; (k) NaOH (aq), THF, ethanol; (l) $PdCl_2$(dppf) (cat), DPPF (cat), DMF, Na_2CO_3 (aq), 80 °C.

dx.doi.org/10.1021/jm301022v | *J. Med. Chem.* 2012, 55, 7920−7939

50% activity of the intracellular calcium responses following stimulation of the cells with the natural ligand agonist, LPA (18:1). As indicated in Table 1, the carboxylic acid is not required for LPA1 inhibition (**3**, **6**, **7**, and **8**). The 2-chloro substitution at the R2 position of the carbamate significantly improved the potency from a partial antagonist (compound **3**) to a full antagonist (compound **6**). Interestingly, the same carbamate moiety was present in both Ki16425 and AM966. Substitution at the 4-position of the phenyl ring (R1 in Table 1) with a methoxy or phenyl group completely abolished LPA1 inhibition potency (**4** and **5**). While the 4-fluorine substitution did not change the potency, the 2-fluorine substitution improved activity by 2- to 3-fold (compare **6** with **7** and **8**). We also observed a stereochemical preference in favor of the (*R*)-enantiomer (compare **8** with **9**), which was consistent with the structure of AM095. When an acetic acid moiety was attached at the 4-position (compound **10**), inhibition of LPA receptor activity was completely lost.

Table 1. SAR of the *N*-Methylpyrazole Derived Non-Carboxylic Acid LPA1 Antagonists 3−10

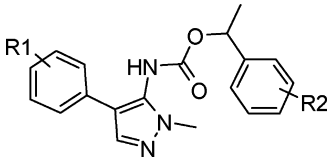

compd	R1	R2	(*R*) or (*S*)	LPA1 IC_{50} (μM)[a]	LPA3 IC_{50} (μM)[a]
3	H	H	(*R*)	17.5 (65%@ 30)[b]	>30
4	4-OCH_3	H	(*R*)	>30	>30
5	4-phenyl	H	(*R*)	>30	>30
6	H	2-Cl	(*R*)/(*S*)	3.59 (>97%@ 30)[b]	>30
7	4-F	2-Cl	(*R*)/(*S*)	3.97 (>97%@ 30)[b]	>30
8	2-F	2-Cl	(*R*)	0.644 (>97%@ 30)[b]	>30
9	2-F	2-Cl	(*S*)	>30	>30
10	4-CH_2COOH	H	(*R*)	>30	>30

[a]Mean value from at least three FLIPR assay IC_{50} determinations; the average CV of the assay was 15%. [b]% inhibition at the indicated concentration.

LPA has been reported to act as a potent mitogenic factor on NHLFs.[7] In order to assess the effects of LPA on the proliferation of NHLFs, we measured the incorporation of nucleoside bromodeoxyuridine (BrdU) into the newly synthesized DNA of NHLFs following stimulation with LPA (18:1). Figure 2A demonstrates that LPA enhanced the proliferation of NHLFs in a concentration-dependent manner (EC_{50} = 12 μM). Since LPA1/2/3 belong to the same EDG family and they share significant structural homology,[25] we applied our selective LPAR antagonists as chemical tools to determine which receptor isoforms were responsible for the NHLF proliferation mediated by LPA (18:1). For NHLF proliferation assays, NHLFs were stimulated with 15 μM LPA (18:1). Compound **1**, a potent LPA2 antagonist (IC_{50} = 17 nM),[22] showed no LPA1 or LPA3 antagonist activity in our FLIPR assay. As displayed in Figure 2B, compound **1** did not reach 50% inhibition even at high compound concentrations (10 μM). Compound **8**, the (*R*)-enantiomer with LPA1 activity in our FLIPR assay (LPA1 IC_{50} = 0.64 μM), inhibited LPA-induced NHLF proliferation more than 50% at 1 μM (IC_{50} = 0.81 μM) and reached complete inhibition at higher concentrations, while the inactive (*S*)-enantiomer, compound **9** (IC_{50} > 30 μM in the LPA1 FLIPR assay), showed significantly less potency (Figure 2B). Taking the combined data from Figure 2A and B, our data strongly suggest that LPA1, and not LPA2, plays a critical role in mediating NHLF proliferation in response to LPA (18:1) addition.

Despite noncarboxylic acid **8** demonstrating reasonable potency in both FLIPR and NHLF proliferation assays, the microsomal instability of this compound (mouse liver microsomal clearance of 89 mL/min/kg and human liver microsomal clearance of 22 mL/min/kg) prevented us using this for *in vivo* studies. After unsuccessful attempts to identify more potent noncarboxylic acid LPA1 antagonists in this chemical class (data not shown), we investigated carboxylic acid analogues of biphenyl substituted aminopyrazoles. Compounds **11**−**20** were studied in the LPA1/3 FLIPR assay (Table 2).

Although direct attachment of an acetic acid moiety at the 4-position of the phenyl group (compound **10**, Table 1) abolished LPA1 activity, and substituting phenyl with a biphenyl resulted in an inactive compound (compound **5**, Table 1), adding an acetic acid to the 4-position of the biphenyl (compound **11**, Table 2) led to a very potent LPA1 antagonist with high selectivity against LPA3 (>850-fold). Replacing the acetic acid with cyclopropanecarboxylic acid gave similar LPA1

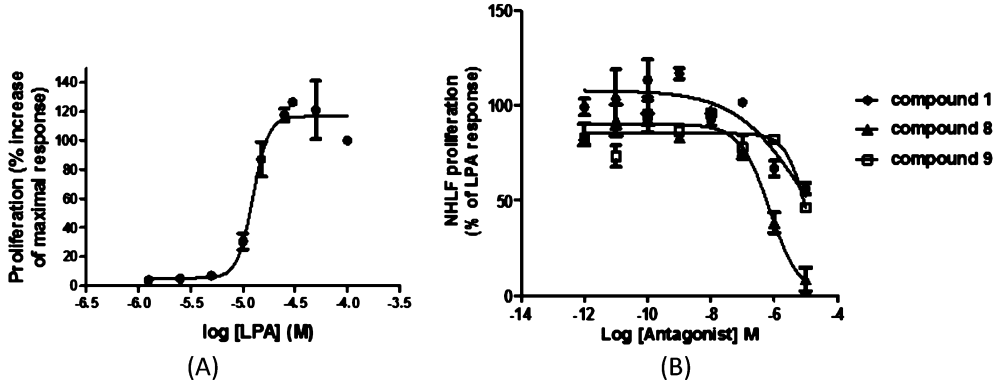

Figure 2. Inhibition of LPA-induced NHLF proliferation by LPA1 and LPA2 antagonists. (A) LPA concentration-dependently increases NHLF proliferation. (B) Effects of compounds **1**, **8**, and **9** on LPA (18:1) (15 μM)-induced NHLF proliferation.

dx.doi.org/10.1021/jm301022v | *J. Med. Chem.* 2012, 55, 7920−7939

Table 2. SAR of the *N*-Methylpyrazole Derived Carboxylic Acid LPA1 Antagonists 11−20

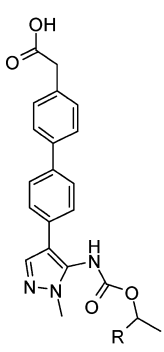

11

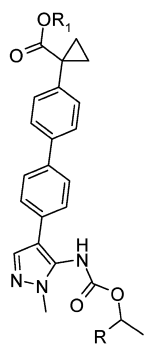

12 (R_1=ethyl), **13-18** (R_1=H)

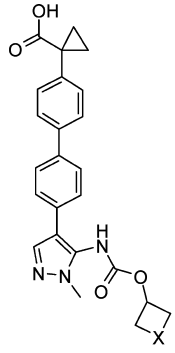

19 (X=CH_2), **20** (X=O)

compd	R	(*R*) or (*S*)	LPA1 IC_{50} (μM)[a]	LPA3 IC_{50} (μM)[a]	BrdU IC_{50} (μM)[b]
11	phenyl	(*R*)	0.035	>30	0.047
12	phenyl	(*R*)	65%@30[c]	>30	ND[d]
13	phenyl	(*R*)	0.021	8.34	0.0026
14	2-F-phenyl	(*R*)	0.024	5.80	0.0045
15	4-F-phenyl	(*R*)/(*S*)	0.057	8.26	0.005
16	3-CF_3-phenyl	(*R*)	0.041	0.478	0.037
17	ethyl	(*R*)	0.038	0% @ 30[c]	0.048
18	isopropyl	(*R*)	0.106	9% @ 30[c]	0.03
19			0.176	13.7% @ 30[c]	0.192
20			0% @ 30[c]	0% @ 30[c]	ND[d]

[a]Mean value from at least three FLIPR assay IC_{50} determinations. [b]NHLF proliferation induced by LPA (18:1) (15 μM) and determined by BrdU incorporation. [c]% inhibition at the indicated concentration. [d]Not determined.

potency but significantly improved antiproliferation activity (compare **11** with **13**). The carboxylic acid was also found to be crucial for LPA1 inhibition (compare **12** with **13**). The improved inhibitory potency in the NHLF proliferation assay observed with the cyclopropanecarboxylic acid prompted us to further study this chemical class. As shown in Table 2, an aryl carbamate is not necessary to maintain LPA1 antagonist potency (R group in Table 2). However, substituting aryl with alkyl groups decreased the inhibitory activity of the series in the NHLF proliferation assay (compare **13** with **17** and **18**). Introduction of polar groups, such as oxetane, caused complete loss of antagonist activity (compare **19** with **20**). Trifluoromethyl substitution at the meta-position significantly increased inhibitory potency in the LPA3 FLIPR assay (17-fold) with little impact on the LPA1 FLIPR assay (compare **13** with **16**). Interestingly, the LPA1/3 dual antagonist **16** was 10-fold less potent than the LPA1-selective antagonist **13** in the NHLF proliferation assay.

To our surprise, the acetic acid derivative of *N*-aryltriazole (compound **21**) showed significantly reduced LPA1 antagonist activity in the FLIPR assays (compare **21** with **11**). However, the corresponding cyclopropanecarboxylic acid analogue (compound **2**) displayed very potent and highly selective inhibitory activity toward LPA1, with little inhibition on LPA3 even at very high concentrations (Table 3). To our knowledge, compound **2** is the most selective nonlipid LPA1 antagonist so far reported in the literature. It appears that compounds from the *N*-aryltriazole chemical class were much more selective for LPA1 than compounds from the corresponding pyrazole series (compare Table 2 with Table 3). Substitution on the phenyl ring of the carbamate or replacing the phenyl group with alkyl groups led to reduced antiproliferative potency (compounds **22**−**28**). In comparison with Ki16425 and AM095, compound **2** showed much improved antiproliferative activity (Figure 4A). The carboxylic acid isosteres **29** and **30** maintained LPA1 potency but were less active in blocking proliferation (compare **29** and **30** with **2** in Table 3). For the heterocyclic triazole core, deletion of the methyl group or substitution with an ethyl group was well tolerated (**31** and **32**). Interestingly, unlike the *N*-aryl-[1,2,3]triazole **32**, the *N*-aryl-[1,2,4]triazole **33** was significantly less active. The observed differences between the two heterocycles can be explained by the stable conformation analysis as illustrated in Scheme 6. It is likely that the NH group in compound **33** exists as the less active conformation due to the unfavorable electronic repulsion. The similar effects of conformational preference due to dipole−dipole interaction on biological activity were reported in GSK3 inhibitors.[26]

To support our conformational analysis, we investigated the differences in the energetic landscapes of the triazole-carbamate torsion angles of **2**, **32**, and **33** through gas-phase density functional theory (DFT) calculations at the B3LYP/6-31G** level. The energy and torsion angle plots revealed that both **32** and **2** have energetic minima at 0° and 40°, respectively, near the orientation shown on the left of Scheme 6 (Figure 3). In contrast, the less active analogue **33** shows a minimum near 100°, where the plane of the carbamate is approximately perpendicular to the plane of the triazole. The difference in energies for **33** between the minimum energy conformation and the conformations with 0° and 40° torsion angles are 4.36 and 3.57 kcal/mol, respectively (Figure 3). These calculations support the hypothesis that differences in conformational preference underlie the differences in activity of **32** and **33**.

Finally, we investigated 1*N*-methyl-4-aryl-[1,2,3]triazole derivatives. As listed in Table 4, unlike *N*-aryl-[1,2,3]triazole **21**, the acetic acid analogue **34** exhibited potent inhibition of LPA1 in the FLIPR assays with good selectivity over LPA3. However, the cyclopropane carboxylic acid analogues displayed much higher potency in inhibiting NHLF proliferation induced by LPA (18:1) (compare **34** with **35** and **36**). Fluorine substitution improved the LPA1 selectivity by 10-fold over LPA3 without affecting the LPA1 potency (compare **35** with **36**). The nonbiaryl acetic acid analogue **43** not only maintained LPA1 inhibitory potency but also displayed high inhibitory activity in blocking LPA-induced NHLF proliferation. The regio-isomeric 1*N*-methyl-5-aryl-[1,2,3]triazole derivative **40** showed significantly less inhibitory activity toward LPA1 or LPA3 in the FLIPR assays. This can also be explained by the unfavorable dipole−dipole interaction that causes the less active conformation as illustrated in Scheme 6.

The most interesting observations were obtained using the LPA1/3 dual antagonists. The trifluoromethyl substitution increased LPA3 inhibition potency by 17-fold without affecting LPA1 inhibitory activity (compare **38** with **35** in Table 4), which is consistent with the data obtained with the corresponding pyrazole analogues (compare **13** and **16** in Table 2). The same trend was observed with *N*-acylsulfonamide analogues (compare **41** with **42** in Table 4). More interestingly, the LPA1/3 dual antagonist was significantly less active than the LPA1-selective antagonist in inhibiting NHLF proliferation mediated by LPA (18:1) despite demonstrating comparable LPA1 inhibitory potency (compare **42** with **41**). This

dx.doi.org/10.1021/jm301022v | *J. Med. Chem.* 2012, 55, 7920−7939

Table 3. SAR of *N*-Aryltriazole Derived LPA1 Antagonists 2 and 21−33

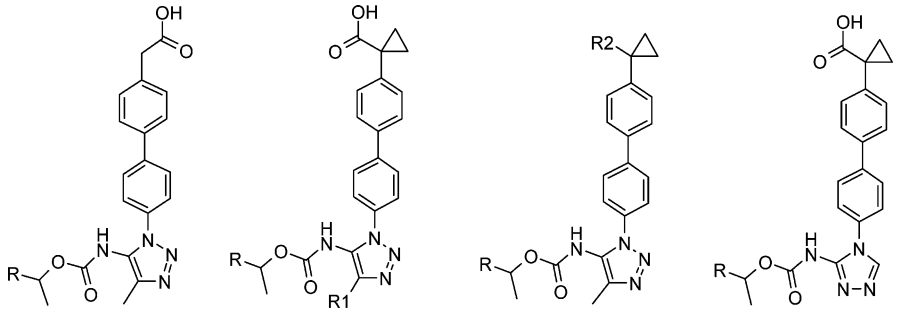

compd	R	(*R*) or (*S*)	LPA1 IC_{50} (μM)[a,c]	LPA3 IC_{50} (μM)[a,c]	BrdU IC_{50} (μM)[b]
21	phenyl	(*R*)	41% @ 30	3% @ 30	ND
2	phenyl	(*R*)	0.0252	20% @ 30	0.004
22	2-F-phenyl	(*R*)	0.0345	42% @ 30	0.021
23	2-CF_3-phenyl	(*R*)	0.112	55% @ 30	0.077
24	3-CF_3-phenyl	(*R*)	0.174	6.86	1.20
25	isopropyl	(*R*)	0.217	17% @ 30	0.060
26	ethyl	(*R*)	0.398	0% @ 30	0.178
27	cyclobutyl	(*R*)/(*S*)	0.161	26% @ 30	0.189
28	gem-dimethyl		0.985	0% @ 30	1.62
29	phenyl	(*R*)	0.032	7% @ 30	0.060
30	phenyl	(*R*)	0.023	28% @ 30	0.105
31	phenyl	(*R*)	0.042	63% @ 30	0.016
32	phenyl	(*R*)	0.036	23% @ 30	0.040
33	phenyl	(*R*)	11% @ 30	17% @ 30	ND[d]

[a]Mean value from at least three FLIPR assay IC_{50} determinations. [b]NHLF proliferation induced by LPA (18:1) (15 μM). [c]% inhibition at the indicated concentration. [d]Not determined.

Scheme 6. Stable Conformation Analysis of 32 and 33

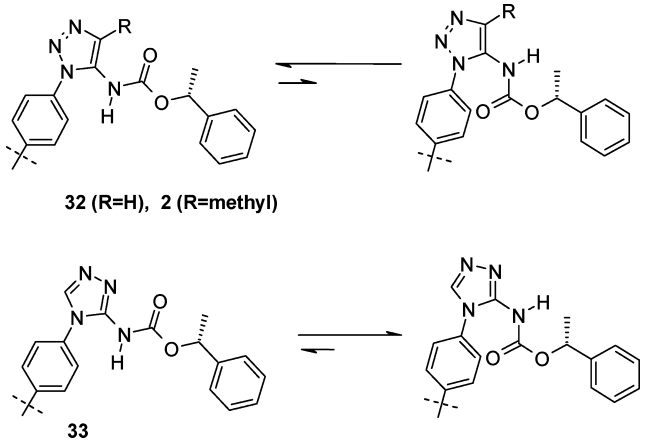

observation may be due to the differential roles of individual LPAR isoforms that effect cellular responses to LPA such as migration and colony formation in soft agar as has been observed in transfected B103 cells.[27] Interestingly, in these studies, LPA1 and LPA3 exhibited opposing effects in B103 cell migration and colony formation in soft agar in response to LPA challenge.[27] It should be noted that in NHLFs we can detect the expression of both LPA1 and LPA3 by quantitative PCR (data not shown). Figure 4B shows the concentration-dependent inhibition of LPA (18:1)-induced NHLF proliferation by LPA1 and LPA1/3 dual antagonists. Taking the results from Tables 1−4 and Figures 2 and 4, we conclude that in

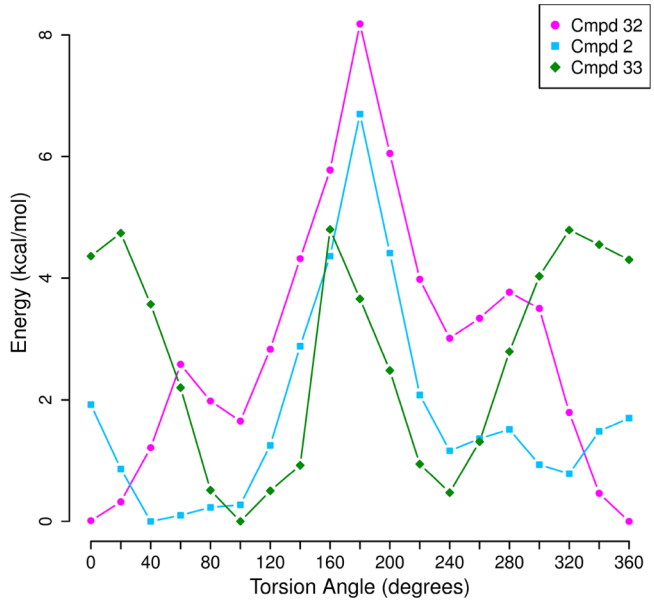

Figure 3. Energy as a function of the triazole-carbamate torsion angle for the [1,2,3]-triazole compound **32** (magenta circles), its active 4-methyl analogue **2** (cyan squares), and the less active [1,2,4]-triazole compound **33** (green diamonds). A torsion angle of 0° or 360° corresponds to the conformations drawn on the left side of Scheme 6, while a torsion angle of 180° corresponds to the conformations drawn on the right side of Scheme 6.

dx.doi.org/10.1021/jm301022v | *J. Med. Chem.* 2012, 55, 7920−7939

Table 4. SAR of *N*-Methyltriazole Derived LPA1 Antagonists 34−43

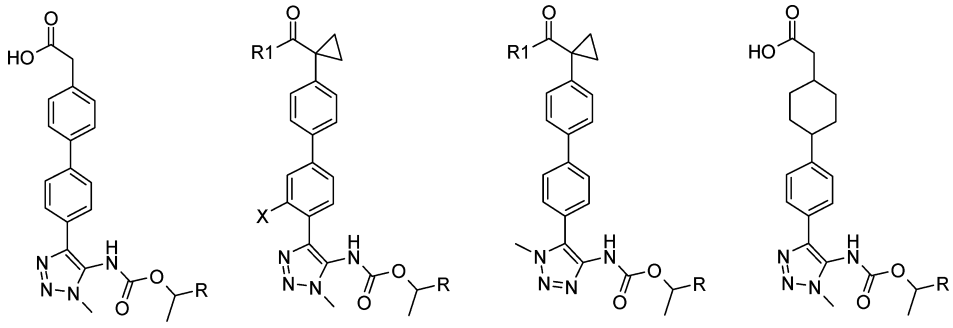

compd	R	R1	(*R*) or (*S*)	LPA1 IC_{50} (μM)[a,c]	LPA3 IC_{50} (μM)[a,c]	BrdU IC_{50} (μM)[b]
34	phenyl		(*R*)	0.048	21.94	0.06
35	phenyl	OH	(*R*)	0.018	2.29	0.003
36	phenyl	OH	(*R*)	0.018	27.35	0.002
37	isopropyl	OH	(*R*)	0.070	24% @ 30	0.020
38	3-CF_3-phenyl	OH	(*R*)	0.017	0.132	0.074
39	3-CF_3-phenyl	OH	(*S*)	2.65	6.30	ND[d]
40	phenyl	OH	(*R*)	12% @ 30	10% @ 30	ND[d]
41	phenyl	CH_3SO_2NH	(*R*)	0.019	2.31	0.004
42	3-CF_3-phenyl	CH_3SO_2NH	(*R*)	0.024	0.065	0.331
43	phenyl		(*R*)	0.058	18.6	0.007

[a]Mean value from at least three FLIPR assay IC_{50} determinations. [b]NHLF proliferation induced by LPA (18:1) (15 μM). [c]% inhibition at the indicated concentration. [d]Not determined.

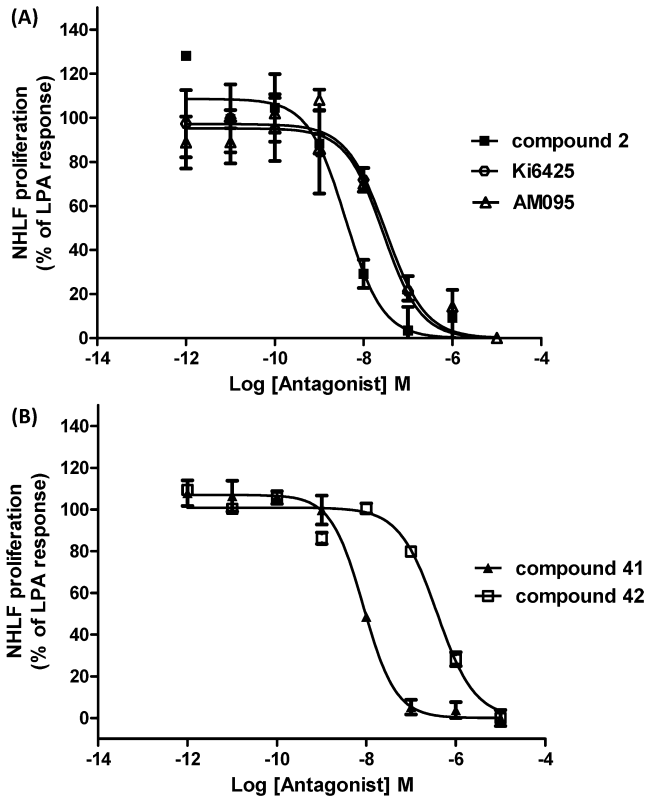

Figure 4. Inhibition of LPA (18:1)-induced NHLF proliferation by LPA1 and LPA1/3 dual antagonists. (A) Concentration-dependent inhibition of LPA (18:1) (15 μM)-stimulated NHLF proliferation by **2**, AM095, and Ki16425. (B) Effects of LPA1 and LPA1/3 dual antagonists (**41** and **42**) on LPA (18:1) (15 μM)-stimulated NHLF proliferation.

NHLFs, LPA (18:1)-induced proliferation is mediated mainly through LPA1 and not LPA2 or LPA3 signaling.

LPA has been reported to act as a contractile agent on NHLFs using the three-dimensional collagen gel contraction assay.[9] Additional studies using lung fibroblasts obtained from the lung of IPF patients suggests that these cells may exhibit elevated expression of contractile proteins and to demonstrate enhanced contraction in three-dimensional collagen gels.[28] We used NHLFs cultured in three-dimensional collagen gels to assess the effect of LPA (18:1) on NHLF contraction. As shown in Figure 5A, LPA concentration-dependently induced contraction of collagen gel matrices containing cultured NHLFs. At concentrations as low as 1 μM, LPA was able to decrease the gel size, with the maximum effect at 30 μM. We next studied the most selective LPA1 antagonist (compound **2**) and the literature LPA2-selective antagonist (compound **1**). Following LPA stimulation (15 μM), the LPA2 antagonist showed no detectable inhibition of the collagen gel contraction, while the LPA1-selective antagonist concentration-dependently inhibited the contraction as shown in Figure 5B. To further determine the relationship between NHLF contraction and proliferation induced by LPA, we evaluated LPA1 and LPA1/3 dual antagonists (compound **41** and **42**). As shown in Figure 5C, the LPA1/3 dual antagonist **42** demonstrated significantly less activity in preventing NHLF contraction than LPA1-selective antagonist **41**. Interestingly, this trend correlated well with LPA-induced NHLF proliferation (Figures 4B and 5C). Therefore, using our novel LPAR antagonists as probes, we have pharmacologically dissected the role of LPA1/2/3 function in mediating LPA-stimulated NHLF proliferation and contraction, processes critical in the progression of lung fibrosis. Table 5 lists the IC_{50} determinations of selected potent LPA1 antagonists in inhibiting NHLF contraction in response to LPA (18:1).

dx.doi.org/10.1021/jm301022v | *J. Med. Chem.* 2012, 55, 7920−7939

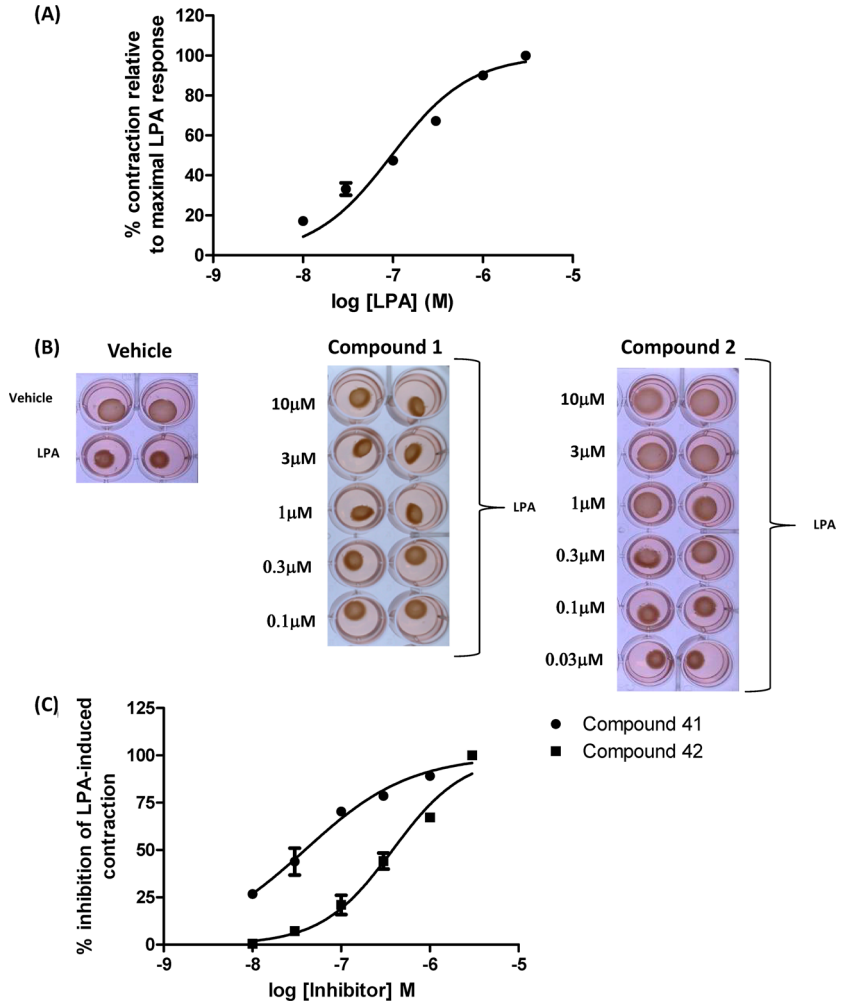

Figure 5. LPA-mediated contraction of NHLFs assessed in three-dimensional collagen gels. (A) LPA (18:1) concentration-dependently increased NHLF contraction. (B) Photo image of the effects of LPAR inhibitors on 15 μM LPA (18:1)-mediated contraction. (C) Effects of LPA1 and LPA1/3 dual antagonists (**41** and **42**) on 15 μM LPA (18:1)-mediated NHLF contraction.

Table 5. IC_{50} Determinations of Selected Potent LPA1 Antagonists in Inhibiting NHLF Contraction in Response to 15 μM LPA (18:1)

compd	inhibition of contraction IC_{50} (μM)[a]
AM095	0.15
Ki16415	0.16
34	0.39
35	0.02
2	0.10
13	0.02
38	0.34
36	0.02
43	0.22

[a]NHLF contraction induced by LPA (18:1) @15 μM.

The unique LPA1 selectivity determined for compound **2** prompted us to evaluate this molecule to inhibit LPA-stimulated histamine release in the mouse, an acute PK/PD model to study LPA1 antagonist activity reported in the literature.[19] As shown in Figure 6A, LPA dose-dependently caused an acute histamine increase in the plasma following intravenous injection. When mice were orally dosed with compound **2** (100 mg/kg, aqueous suspension) prior to intravenous LPA injection, the LPA-induced histamine level was significantly blocked (Figure 6B). A clear PK/PD relationship was demonstrated by the correlation between the levels of compound **2** and LPA-induced histamine concentrations in plasma (Figure 6C). Although AM095 almost completely blocked histamine release (100 mg/kg), analysis of plasma samples revealed more than 65-fold higher concentrations of AM095 than compound **2** (100 mg/kg). The ability of compound **2** to block histamine release at much lower plasma concentration suggests that further improvement of pharmacokinetic properties of this chemical class could lower the effective dose.

IPF represents a disease of enormous unmet medical need due to the lack of effective treatment options and the dismal prognosis associated with the disease. Preclinical and clinical data exist that support targeting LPA1 for the treatment of organ fibrosis including IPF due to the role of this receptor in mediating the profibrotic effects of LPA in fibroblasts.[7,8,11] More recently, it has been reported that LPA acting through the LPA1 receptor isoform may induce apoptosis of human bronchial epithelial cells suggesting that LPA1 may promote lung fibrosis in cell types other than pulmonary fibroblasts.[29] In this work, we have used our novel LPA1, LPA1/3 dual, and literature LPA2 antagonists as chemical probes to pharmaco-

dx.doi.org/10.1021/jm301022v | J. Med. Chem. 2012, 55, 7920−7939

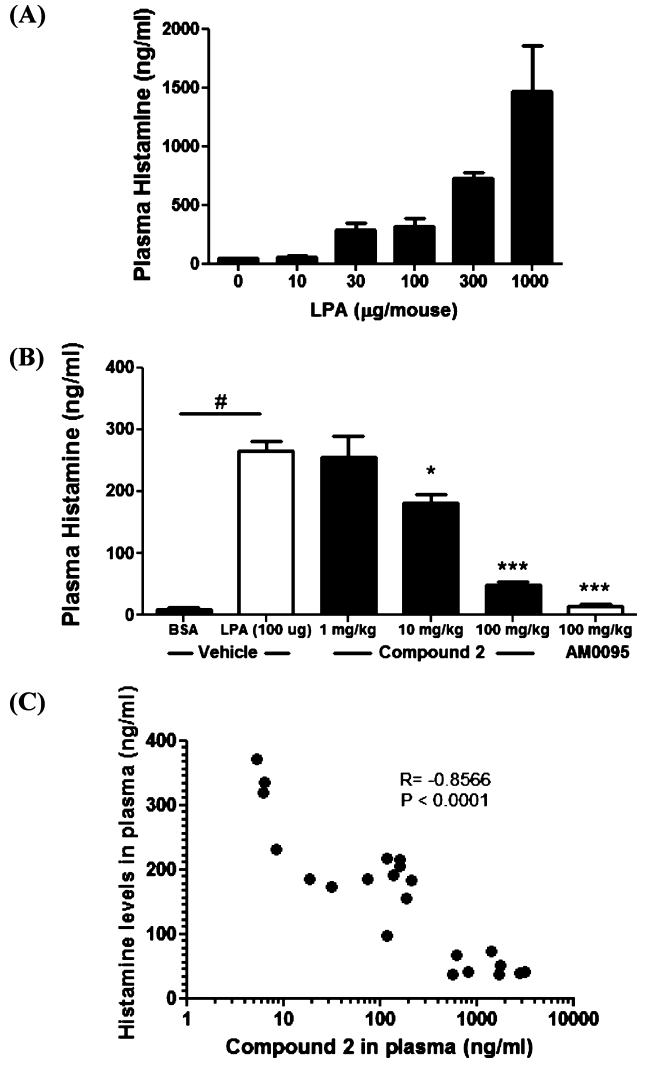

Figure 6. LPA-induced histamine release in C57BL/6 mice. (A) LPA (intravenous injection) dose-dependently increased plasma histamine levels. (B) Dose-dependent inhibition of LPA-mediated plasma histamine levels by orally dosed compound **2**. (C) Correlation of histamine levels with compound **2** concentrations in plasma. Significance is denoted as follows: * $p < 0.05$, ** $p < 0.01$, and *** $p < 0.001$.

logically dissect the function of LPA1/2/3 in driving LPA-mediated profibrotic responses in NHLFs. Our data suggests that the LPA1 receptor is the predominant receptor for mediating LPA-induced NHLF proliferation and contraction, critical cellular responses implicated in the progression of IPF.

Since the first publication of the isoxazole-derived LPAR antagonist, Ki16425 in 2003, the majority of nonlipid LPA1 antagonists disclosed in patent applications or published in the literature are still based on the isoxazole core structure.[30,31] By taking bioisostere approaches, we discovered pyrazole and triazole-derived LPA1 selective and LPA1/3 dual antagonists. Compound **2** demonstrated the highest LPA1 selectivity and attenuated LPA-induced NHLF proliferation and contraction with high potency. Oral dosing of compound **2** in mice caused a dose-dependent reduction in serum histamine levels induced following intravenous LPA stimulation. The carboxylic acid-derived LPA1 antagonists from our pyrazole and triazole chemical class showed no liability to CYP, hERG, and other *in vitro* predictive toxicity assays. The correlation between the inhibition of LPA-induced NHLF proliferation and the inhibition of LPA-induced NHLF contraction by our novel LPA1 antagonists further underscore that LPA1 represents a potentially attractive therapeutic target for the treatment of IPF.

EXPERIMENTAL SECTION

All reactions were carried out under an argon atmosphere. Solvents were purchased from commercial sources and used without further drying. ^{1}H NMR spectra were recorded with Mercury 300 and Unityplus 400 MHz spectrometers. All compounds were analyzed by LC/MS (liquid chromatography/mass spectrometry) using a Waters ZQ mass detector and Waters LC system. Ionization was generally achieved via electron spray (ES). The LC fraction detection consisted of both a diode array detector and an evaporative light scattering detector, and all tested compounds had purity greater than 98%.

[4-(2-Fluoro-phenyl)-2-methyl-2*H*-pyrazol-3-yl]-carbamic Acid (*R*)-1-(2-Chloro-phenyl)-ethyl Ester (8). 4-Bromo-1-methyl-1*H*-pyrazol-5-amine (800 mg, 4.55 mmol), 2-fluorophenylboronic acid (890 mg, 6.36 mmol), X-Phos (217 mg, 0.45 mmol), palladium acetate (51 mg, 0.227 mmol), and potassium phosphate tribasic (1.93 g, 9.09 mmol) were combined in 12 mL of toluene. Degassed water (4 mL) was added, and argon was bubbled through for 3 min. The reaction tube was sealed, and the mixture was stirred at 95 °C overnight. Solvents were evaporated, and the residue was extracted with ethyl acetate and water. The organic layer was washed with brine and dried. Solvents were evaporated, and the residue was purified by flash column chromatography (ethyl acetate containing 3% methanol in hexanes 10% to 80%) to give 4-(2-fluorophenyl)-2-methyl-2*H*-pyrazole-3-amine as a brown oil (649 mg, 74.7% yield). ^{1}H NMR (DMSO-d_6) δ ppm 3.60 (s, 3H), 5.30 (br s, 2H), 7.14−7.25 (m, 3H), 7.30 (d, J = 2.5 Hz, 1H), 7.39−7.52 (m, 1H); LC/MS calcd for $C_{10}H_{10}FN_3$ (m/e) 191.0; obsd, 192.0 (M + H, ES$^+$).

4-(2-Fluorophenyl)-2-methyl-2*H*-pyrazol-3-amine (110 mg, 0.575 mmol) and triphosgene (222 mg, 0.748 mmol) were combined with dichloromethane (4 mL) and toluene (6 mL). The reaction tube was sealed. The mixture was stirred in an ice bath, and triethylamine (0.7 mL) was added. The mixture was stirred at 85 °C for 20 min, and 1-(2-chlorophenyl)ethanol (117 mg, 0.748 mmol) in 1 mL of toluene was added. The mixture was stirred at 90 °C for 1 h. Solvents were evaporated, and the residue was extracted with ethyl acetate and water. The organic layer was dried and concentrated. The residue was purified by flash column chromatography (ethyl acetate in hexanes 0% to 50%) to give [4-(2-fluoro-phenyl)-2-methyl-2*H*-pyrazol-3-yl]-carbamic acid 1-(2-chloro-phenyl)-ethyl ester as an amorphous powder (134 mg, 62.3% yield). ^{1}H NMR (DMSO-d_6) δ ppm 1.06−1.28 (m, 1H), 1.53 (br d, J = 5.6 Hz, 2H), 3.65 (br s, 3H), 5.83−5.98 (m, 1H), 6.83−7.50 (m, 7H), 7.56 (d, J = 6.8 Hz, 1H), 7.65 (br s, 1H), 9.66 (s, 1H); LC/MS calcd for $C_{19}H_{17}ClFN_3O_2$ (m/e) 373.0; obsd, 372.0 (M − H, ES$^-$). This pure racemic material was separated by supercritical fluid chromatography using a chiral WHELKO column (10% to 65% methanol in CO_2, 70 mL/min). The second fraction (longer retention time) was concentrated to give a pure enantiomer as compound **8**.

[4-(2-Fluoro-phenyl)-2-methyl-2*H*-pyrazol-3-yl]-carbamic Acid (*S*)-1-(2-Chloro-phenyl)-ethyl Ester (9). The first fraction from the chiral SFC separation of [4-(2-fluoro-phenyl)-2-methyl-2*H*-pyrazol-3-yl]-carbamic acid 1-(2-chloro-phenyl)-ethyl ester as described for the preparation of **8** gave a pure enantiomer as compound **9**.

2-Methyl-4-phenyl-2*H*-pyrazol-3-yl-carbamic Acid (*R*)-1-Phenyl-ethyl Ester (3). Methyl 4-bromo-2-methyl-2*H*-pyrazole-3-carboxylate (438.1 mg, 2.0 mmol), phenylboronic acid (244 mg, 2.0 mmol), and cesium carbonate (1.3 g, 4.0 mmol) were dissolved in 10 mL of DMF, and the solution was degassed with argon. To this mixture was added $Pd(PPh_3)_4$ (139 mg, 0.12 mmol). The mixture was stirred at 80 °C for 12 h. The resulting mixture was cooled to room temperature and filtered. The solid was rinsed with THF. The filtrate was concentrated and purified by ISCO flash column chromatography (0% to 25% ethyl acetate in hexanes) to give an oily material as methyl

dx.doi.org/10.1021/jm301022v | *J. Med. Chem.* 2012, 55, 7920−7939

2-methyl-4-phenyl-2*H*-pyrazole-3-carboxylate (388.6 mg, 89.8% yield). ^{1}H NMR ($CDCl_3$) δ ppm 3.77 (s, 3H), 4.21 (s, 3H), 7.31−7.36 (m, 1H), 7.37−7.42 (m, 4H), 7.52 (s, 1H); LC/MS calcd for $C_{12}H_{12}N_2O_2$ 216.0; obsd, 217.0 (M + H, ES$^+$).

Methyl 2-methyl-4-phenyl-2*H*-pyrazole-3-carboxylate (388.6 mg, 1.8 mmol) was dissolved in THF (8 mL), and 0.5 N LiOH solution (4 mL) was added. The mixture was stirred at 60 °C for 2 h and then concentrated. The residue was dissolved in water (30 mL) and filtered. The filtrate was neutralized with 1 N hydrochloric acid, and the white precipitate was filtered and dried in a vacuum oven at 60 °C overnight to provide 2-methyl-4-phenyl-2*H*-pyrazole-3-carboxylic acid (338.5 mg, 93.1% yield). ^{1}H NMR (DMSO-d_6) δ ppm 4.06 (s, 3H), 7.25−7.42 (m, 5H), 7.60 (s, 1H), 13.42 (s, 1H); LC/MS calcd for $C_{11}H_{10}N_2O_2$ 202.0; obsd, 201.0 (M − H, ES$^-$).

2-Methyl-4-phenyl-2*H*-pyrazole-3-carboxylic acid (100 mg, 0.495 mmol), (*R*)-1-phenylethanol (60.4 mg, 0.495 mmol), DPPA (136 mg, 0.495 mmol), and TEA (100 mg, 0.989 mmol) were mixed with 3 mL of toluene. The mixture was stirred at 80 °C for 1 h. Solvents were evaporated, and the residue was purified by ISCO flash column chromatography (0% to 55% ethyl acetate in hexanes) to give 2-methyl-4-phenyl-2*H*-pyrazol-3-yl-carbamic acid (*R*)-1-phenyl-ethyl ester as a white powder (106 mg, 66.7% yield). ^{1}H NMR (DMSO-d_6) δ ppm 1.13−1.29 (br, 1 H), 1.52 (d, J = 5.8 Hz, 2 H), 3.60 (s, 3H), 5.58−5.82 (br m, 1H), 6.92−7.53 (m, 10H), 7.74 (s, 1H), 9.55 (s, 1H); LC/MS calcd for $C_{19}H_{19}N_3O_2$ 321.0; obsd, 320.0 (M − H, ES$^-$).

Compounds **4** to **7** were prepared using the same procedure as that for the preparation of compound **3**.

[4-(4-Methoxy-phenyl)-2-methyl-2*H*-pyrazol-3-yl]-carbamic Acid (*R*)-1-Phenyl-ethyl Ester (4). ^{1}H NMR (DMSO-d_6) δ ppm 1.15−1.30 (br, 1H), 1.54 (d, J = 5.8 Hz, 2 H), 3.60 (br s, 3H), 3.75 (s, 3H), 5.76 (d, J = 6.1 Hz, 1H), 6.87 (d, J = 7.6 Hz, 2H), 6.97−7.25 (m, 1H), 7.28−7.51 (m, 6H), 7.67 (s, 1H), 9.48 (br s, 1H); LC/MS calcd for $C_{25}H_{23}N_3O_2$ (m/e) 397; obsd, 398.0 (M + H, ES+); LC/MS calcd for $C_{20}H_{21}N_3O_3$ (m/e) 351; obsd, 350.0 (M − H, ES$^-$).

(4-Biphenyl-4-yl-2-methyl-2*H*-pyrazol-3-yl)-carbamic Acid (*R*)-1-Phenyl-ethyl Ester (5). ^{1}H NMR (DMSO-d_6) δ ppm 1.12−1.30 (br, 1H), 1.57 (d, J = 5.8 Hz, 2 H), 3.64 (br s, 3H), 5.79 (d, J = 5.8 Hz, 1H), 7.29−7.51 (m, 8H), 7.52−7.58 (m, 2H), 7.59−7.65 (m, 2H), 7.68 (d, J = 7.6 Hz, 2H), 7.83 (s, 1H), 9.63 (br s, 1H); LC/MS calcd for $C_{25}H_{23}N_3O_2$ (m/e) 397; obsd, 398.0 (M + H, ES$^+$).

(2-Methyl-4-phenyl-2*H*-pyrazol-3-yl)-carbamic Acid 1-(2-Chloro-phenyl)-ethyl Ester (6). 2-Methyl-4-phenyl-2*H*-pyrazole-3-carboxylic acid (60 mg, 0.297 mmol), 1-(2-chlorophenyl)ethanol (46.5 mg, 0.297 mmol), DPPA (81.7 mg, 0.297 mmol), and triethylamine (0.09 mL) were combined in 2.5 mL of toluene. The mixture was stirred at 85 °C for 3 h. Solvents were evaporated, and the residue was purified by flash column chromatography (0% to 50% ethyl acetate in hexanes) to give (2-methyl-4-phenyl-2*H*-pyrazol-3-yl)-carbamic acid 1-(2-chloro-phenyl)-ethyl ester as a white fluffy solid (40 mg, 38% yield). ^{1}H NMR (DMSO-d_6) δ ppm 1.15−1.28 (br, 1H), 1.55 (d, J = 5.8 Hz, 2H), 3.54−3.78 (m, 3H), 5.82−6.10 (m, 1H), 7.23 (d, J = 6.8 Hz, 1H), 7.28−7.54 (m, 7H), 7.59 (d, J = 6.8 Hz, 1H), 7.76 (br s, 1H), 9.68 (s, 1H). LC/MS calcd for $C_{19}H_{18}ClN_3O_2$ (m/e) 355.0; obsd, 356.0 (M + H, ES$^+$).

[4-(4-Fluoro-phenyl)-2-methyl-2*H*-pyrazol-3-yl]-carbamic Acid 1-(2-Chloro-phenyl)-ethyl Ester (7). ^{1}H NMR (DMSO-d_6) δ ppm 1.15−1.30 (br, 1H), 1.56 (br d, J = 5.3 Hz, 2H), 3.62 (br s, 3H), 5.86−6.06 (m, 1H), 6.81−7.27 (m, 3H), 7.31−7.65 (m, 5H), 7.76 (br s, 1H), 9.65 (s, 1H); LC/MS calcd for $C_{19}H_{17}ClFN_3O_2$ (m/e) 373.0; obsd, 374.0 (M + H, ES$^+$).

{4-[1-Methyl-5-((*R*)-1-phenyl-ethoxycarbonylamino)-1*H*-Pyrazol-4-yl]-phenyl}-acetic Acid (10). 4-Bromo-2-methyl-2*H*-pyrazole-3-carboxylic acid (787.2 mg, 3.84 mmol), DPPA (1.16 g, 4.22 mmol), (*R*)-1-phenylethanol (491 mg, 4.02 mmol), and TEA (1.10 mL, 7.68 mmol) were combined in 15 mL of toluene to give a clear solution. The mixture was heated to 80 °C and stirred for 1 h. Solvents were evaporated, and the residue was extracted with ethyl acetate and sodium bicarbonate solution. The organic layer was dried and evaporated to give an oily material (1.38 g). ^{1}H NMR of the crude material indicated 75% of the desired compound as 4-bromo-2-methyl-2*H*-pyrazol-3-yl-carbamic acid (*R*)-1-phenyl-ethyl ester (**45**). LRMS calcd for $C_{13}H_{14}BrN_3O_2$ (m/e) 324.0; obsd, 323.0 (M − H, ES$^-$).

4-Bromo-2-methyl-2*H*-pyrazol-3-yl-carbamic acid (*R*)-1-phenyl-ethyl ester (263.5 mg, 0.61 mmol), ethyl 1-(4-(4,4,5,5-tetramethyl-1,3,2-dioxaborolan-2-yl)-phenyl)-acetate (354 mg, 1.22 mmol), X-Phos (116 mg, 0.244 mmol), and palladium acetate (27.4 mg, 0.122 mmol) were dissolved in toluene (6 mL), and potassium phosphate tribasic (518 mg, 2.44 mmol) in degassed water (1.5 mL) was added. The mixture was degassed for 5 min and sealed. The mixture was stirred at 100 °C for 4 h and then extracted with ethyl acetate and water. The organic layer was washed with brine and dried. Solvents were evaporated, and the residue was purified by ISCO flash column chromatography using ethyl acetate in hexanes (0% to 50%) to give a waxy pale yellow material as {4-[1-methyl-5-((*R*)-1-phenyl-ethoxycarbonylamino)-1*H*-pyrazol-4-yl]-phenyl}-acetic acid ethyl ester (134 mg, 54% yield). LC/MS calcd for $C_{23}H_{25}N_3O_4$ (m/e) 407.0; obsd, 408.0 (M + H, ES$^+$).

{4-[1-Methyl-5-((*R*)-1-phenyl-ethoxycarbonylamino)-1*H*-pyrazol-4-yl]-phenyl}-acetic acid ethyl ester (134 mg, 0.33 mmol) was dissolved in THF (4 mL), and aqueous lithium hydroxide solution (0.5N, 1 mL) was added. The reaction was stirred for 6 h. Solvents were evaporated, and the residue was treated with water (15 mL) to give a clear solution followed by the addition of 1 N hydrochloric acid (0.55 mL). The white solid was filtered and rinsed with water and dried in air to give {4-[1-methyl-5-((*R*)-1-phenyl-ethoxycarbonylamino)-1*H*-pyrazol-4-yl]-phenyl}-acetic acid (90 mg, 72% yield). ^{1}H NMR (DMSO-d_6) δ ppm 1.48 (br s, 3H), 3.48 (s, 2H), 3.54 (s, 3H), 5.70 (d, J = 5.6 Hz, 1H), 7.06−7.42 (m, 9H), 7.67 (s, 1H), 9.48 (br s, 1H), 12.28 (br s, 1H); LC/MS calcd for $C_{21}H_{21}N_3O_4$ (m/e) 379.0; obsd, 380.0 (M + H, ES$^+$).

{4′-[1-Methyl-5-((*R*)-1-phenyl-ethoxycarbonylamino)-1*H*-pyrazol-4-yl]-biphenyl-4-yl}-acetic Acid (11). Ethyl 2-(4-bromophenyl)-acetate (2.43 g, 10 mmol), 4-hydroxyphenylboronic acid (1.65 g, 12 mmol), $Pd(PPh_3)_4$ (693 mg, 0.6 mmol), and potassium carbonate (2.76 g, 20 mmol) were combined in 14 mL of dry DMF. The mixture was bubbled with nitrogen and sealed. The mixture was stirred at 85 °C for 15 h. Solvents were evaporated, and the residue was extracted with ethyl acetate and water. The organic layer was washed with brine and dried over sodium sulfate. Solvents were evaporated, and the residue was purified by flash column chromatography (5% to 50% ethyl acetate in hexanes). The pure fraction was combined and concentrated. The residue was dissolved in ethyl acetate (4 mL), and hot hexanes were added. The white solid was filtered and dried to give 4′-hydroxy-biphenyl-4-yl-acetic acid ethyl ester (1.68 g, 65.6% yield). ^{1}H NMR ($CDCl_3$) δ ppm 1.29 (t, J = 7.1 Hz, 3H), 3.66 (s, 2H), 4.19 (q, J = 7.1 Hz, 2H), 4.95 (br. s., 1 H), 6.87 (d, J = 8.6 Hz, 2H), 7.33 (d, J = 8.3 Hz, 2H), 7.47 (m, 4H); LC/MS calcd for $C_{16}H_{16}O_3$ (m/e) 256.0; obsd, 257.1 (M + H, ES$^+$).

4′-Hydroxy-biphenyl-4-yl-acetic acid ethyl ester (641 mg, 2.5 mmol) was dissolved in dichloromethane (15 mL). To this solution was added trifluoromethanesulfonic anhydride (706 mg, 2.5 mmol) at −78 °C. Triethylamine (0.35 mL, 2.5 mmol) was added. The mixture was stirred at −78 °C for 10 min and warmed to room temperature. After 30 min, the mixture was extracted with water and methylene chloride. The organic layer was washed with diluted hydrochloric acid and concentrated sodium bicarbonate solution. Solvents were evaporated, and the residue was treated with hexanes. The gray crystalline material was filtered to give 4′-trifluoromethanesulfonyloxy-biphenyl-4-yl-acetic acid ethyl ester (812 mg, 83.6% yield). ^{1}H NMR ($CDCl_3$) δ ppm 1.29 (t, J = 7.1 Hz, 3H), 3.68 (s, 2H), 4.19 (q, J = 7.1 Hz, 2H), 7.35 (d, J = 8.1 Hz, 2H), 7.39 (d, J = 8.1 Hz, 2H), 7.53 (d, J = 8.0 Hz, 2H), 7.64 (d, J = 8.0 Hz, 2H).

4′-Trifluoromethanesulfonyloxy-biphenyl-4-yl-acetic acid ethyl ester (800 mg, 2.06 mmol), 4,4,4′,4′,5,5,5′,5′-octamethyl-2,2′-bi(1,3,2-dioxaborolane) (628 mg, 2.47 mmol), potassium acetate (607 mg, 6.18 mmol), and Pd(dppf)Cl_2 (90.4 mg, 0.124 mmol) were combined in dry dioxane (15 mL). The mixture was stirred with argon bubbled through for 5 min. The mixture was heated to 90 °C and stirred for 4 h. The resulting material was filtered through a layer of silica gel and rinsed with ethyl acetate. Solvents were evaporated, and the residue

dx.doi.org/10.1021/jm301022v | *J. Med. Chem.* 2012, 55, 7920−7939

was purified by flash column chromatography (0% to 30% ethyl acetate in hexanes) to give [4′-(4,4,5,5-tetramethyl-[1,3,2]-dioxaborolan-2-yl)-biphenyl-4-yl]-acetic acid ethyl ester as a white solid (728 mg, 96.5% yield). ^{1}H NMR ($CDCl_3$) δ ppm 1.28 (t, J = 7.1 Hz, 3H), 1.37 (s, 12H), 3.67 (s, 2H), 4.18 (q, J = 7.1 Hz, 2H), 7.37 (d, J = 8.1 Hz, 2H), 7.60 (dd, J = 8.0, 6.4 Hz, 4H), 7.88 (d, J = 8.1 Hz, 2H).

In a 50 mL round-bottom flask, palladium acetate (12.5 mg, 0.055 mmol), X-Phos (52.9 mg, 0.11 mmol), and potassium phosphate tribasic (236 mg, 1.11 mmol) were mixed in 0.5 mL of degassed water and 1 mL of toluene and stirred for 1 min. Then 4-bromo-2-methyl-2*H*-pyrazol-3-yl-carbamic acid (*R*)-1-phenyl-ethyl ester (180 mg, 0.55 mmol) in 2 mL of toluene was added followed by the addition of [4′-(4,4,5,5-tetramethyl-[1,3,2]dioxaborolan-2-yl)-biphenyl-4-yl]-acetic acid ethyl ester (203 mg, 0.55 mmol) and 1 mL of toluene. The mixture was degassed with argon and sealed. The mixture was stirred at 95 °C overnight. The resulting mixture was extracted with ethyl acetate and water. The organic layer was dried and evaporated. The residue was purified by flash column chromatography (ethyl acetate with 5% methanol in hexanes) to give {4′-[1-methyl-5-((*R*)-1-phenyl-ethoxycarbonylamino)-1*H*-pyrazol-4-yl]-biphenyl-4-yl}-acetic acid ethyl ester (78.0 mg, 29.1% yield) as an amorphous material. LC/MS calcd for $C_{29}H_{29}N_3O_4$ (m/e) 483.0; obsd, 484.1 (M + H, ES$^+$). This material was dissolved in 6 mL of THF, and lithium hydroxide solution (1 mL, 0.5 N) was added followed by 0.2 mL of methanol. The mixture was stirred at room temperature for 4 h and concentrated. Warm water (35 mL) was added, and the mixture was filtered. The filtrate was acidified with 1 N hydrochloric acid (0.6 mL) and filtered. The solid was dried under vacuum overnight to give a pale yellow solid as {4′-[1-methyl-5-((*R*)-1-phenyl-ethoxycarbonylamino)-1*H*-pyrazol-4-yl]-biphenyl-4-yl}-acetic acid (30 mg, 40.8% yield). ^{1}H NMR (DMSO-d_6) δ ppm 1.15−1.32 (br, 1H), 1.56 (d, J = 5.8 Hz, 2H), 3.62 (s, 2H), 3.63 (s, 3H), 5.66−5.83 (br m, 1H), 7.03 (br, 0.5H), 7.18 (br, 0.5H), 7.28−7.38 (m, 3H), 7.38−7.48 (m, 3H), 7.49−7.56 (m, 1H), 7.57−7.68 (m, 5H), 7.81 (s, 1H), 9.62 (s, 1H), 12.38 (s, 1H); LC/MS calcd for $C_{27}H_{25}N_3O_4$ (m/e) 455.0; obsd, 456.0 (M + H, ES$^+$).

1-{4′-[1-Methyl-5-((*R*)-1-phenyl-ethoxycarbonylamino)-1*H*-pyrazol-4-yl]-biphenyl-4-yl}-cyclopropanecarboxylic Acid Ethyl Ester (12). Ethyl 1-(4′-(4,4,5,5-tetramethyl-1,3,2-dioxaborolan-2-yl)-biphenyl-4-yl)-cyclopropanecarboxylate (100 mg, 0.255 mmol), 4-bromo-1-methyl-1*H*-pyrazol-5-amine (67.3 mg, 0.38 mmol), X-Phos (36.5 mg, 0.077 mol), potassium phosphate tribasic (162 mg, 0.76 mmol), and palladium acetate (8.6 mg, 0.038 mmol) were mixed in 4 mL of toluene. The mixture was stirred, and degassed water (0.8 mL) was added. The mixture was degassed with nitrogen and sealed. The mixture was stirred at 100 °C overnight and then extracted with ethyl acetate and water. Solvents were evaporated, and the residue was purified by flash column chromatography (methanol in methylene chloride 0% to 10%) to give a pale gray solid as 1-[4′-(5-amino-1-methyl-1*H*-pyrazol-4-yl)-biphenyl-4-yl]-cyclopropanecarboxylic acid ethyl ester (48 mg, 52.1% yield). ^{1}H NMR ($CDCl_3$) δ ppm 1.19−1.25 (m, 5H), 1.64 (m, 2H), 3.77 (s, 3H), 3.81(br s, 2H), 4.13 (q, J = 7.1 Hz, 2H), 7.44 (t, J = 8.8 Hz, 4H), 7.53 (s, 1H), 7.56 (d, J = 8.1 Hz, 2H), 7.64 (d, J = 8.1 Hz, 2H); LC/MS calcd for $C_{22}H_{23}N_3O_2$ (m/e) 361.0; obsd, 362.1 (M + H, ES$^+$).

1-[4′-(5-Amino-1-methyl-1*H*-pyrazol-4-yl)-biphenyl-4-yl]-cyclopropanecarboxylic acid ethyl ester (100 mg, 0.277 mmol) and triphosgene (123 mg, 0.415 mmol) were dissolved in methylene chloride (2 mL) to give a solution. Toluene (6 mL) was added, and the mixture was stirred followed by the addition of TEA (0.16 mL). The mixture was sealed and stirred at 90 °C for 10 min. (*R*)-(+)-1-Phenylethanol (68 mg, 0.553 mmol) in toluene (2 mL) was added. The mixture was stirred at 85 °C for 2 h. This material was extracted with ethyl acetate and ammonium chloride solution. The organic layer was dried over sodium sulfate and filtered. Solvents were evaporated, and the residue was purified by flash column chromatography (0% to 60% ethyl acetate in hexanes) to give a gray powder as 1-{4′-[1-methyl-5-((*R*)-1-phenyl-ethoxycarbonylamino)-1*H*-pyrazol-4-yl]-biphenyl-4-yl}-cyclopropanecarboxylic acid ethyl ester (101 mg, 71.6% yield). ^{1}H NMR ($CDCl_3$) δ ppm 1.20−1.34 (m, 6H), 1.49−1.75 (m, 4H), 3.80 (s, 3H), 4.14 (q, J = 7.1 Hz, 2H), 5.93 (m, 1H), 6.25 (br s, 1H), 7.35−7.48 (m, 9H), 7.53−7.64 (m, 4H), 7.72 (s, 1H); LC/MS calcd for $C_{31}H_{31}N_3O_4$ (m/e) 509.0; obsd, 510.0 (M + H, ES$^+$).

1-{4′-[1-Methyl-5-((*R*)-1-phenyl-ethoxycarbonylamino)-1*H*-pyrazol-4-yl]-biphenyl-4-yl}-cyclopropanecarboxylic acid (13). 1-{4′-[1-Methyl-5-((*R*)-1-phenyl-ethoxycarbonylamino)-1*H*-pyrazol-4-yl]-biphenyl-4-yl}-cyclopropanecarboxylic acid ethyl ester (80 mg, 0.157 mmol) was dissolved in 4 mL of THF, and lithium hydroxide solution (0.5N, 2 mL) was added. The mixture was stirred at room temperature for 5 min. Methanol (1 mL) was added to give a clear solution. The mixture was stirred at 65 °C for 5 h and then at 30 °C overnight. Solvents were evaporated, and the residue was dissolved in water (12 mL). Hydrochloric acid (1 N, 1.3 mL) was added, and the solid was filtered to give a white solid (65 mg). LC/MS indicated 85% purity with the major impurity as the cleavage of carbamate. This solid was dissolved in acetonitrile/methylene chloride (containing 5% methanol) and purified by flash column chromatography (methanol in dichloromethane 0% to 5%) to give a white solid as 1-{4′-[1-methyl-5-((*R*)-1-phenyl-ethoxycarbonylamino)-1*H*-pyrazol-4-yl]-biphenyl-4-yl}-cyclopropanecarboxylic acid (45 mg, 59.5% yield). ^{1}H NMR (DMSO-d_6) δ ppm 1.19−1.25 (m, 2H), 1.49−1.57 (m, 5H), 3.64 (s, 3H), 5.65−5.83 (m, 1H), 6.95−7.25 (br m, 1H), 7.27−7.48 (m, 6H), 7.49−7.67 (m, 6H), 7.82 (br s, 1H), 9.25 (br s, 0.2H), 9.57 (s, 0.8H), 12.35 (s, 1H); LC/MS calcd for $C_{29}H_{27}N_3O_4$ (m/e) 481.0; obsd, 482.1 (M + H, ES$^+$).

Compounds **14**−**20** were prepared with the same method described for the preparation of compound **13**.

(*R*)-1-{4′-[5-((1-(2-Fluorophenyl)ethoxy)carbonylamino)-1-methyl-1*H*-pyrazol- 4-yl]-biphenyl-4-yl}-cyclopropanecarboxylic Acid (14). ^{1}H NMR (DMSO-d_6) δ ppm 12.37 (br. s., 1H), 9.67 (s, 1H), 7.80 (s, 2H), 7.45−7.70 (m, 8H), 7.39 (d, 2H), 7.19−7.33 (m, 1H), 5.97 (d, J = 5.7 Hz, 1H), 3.62 (s, 3H), 1.57 (m, 2H), 1.38−1.52 (m, 2H), 1.22 (s, 1H), 1.15 (d, 2H); LC/MS calcd for $C_{29}H_{26}FN_3O_4$ (m/e) 499.0; obsd, 500.1 (M + H, ES$^+$).

1-{4′-[5-((1-(4-Fluorophenyl)ethoxy)carbonylamino)-1-methyl-1*H*-pyrazol- 4-yl]-biphenyl-4-yl}-cyclopropanecarboxylic Acid (15). ^{1}H NMR (DMSO-d_6) δ ppm 12.36 (br. s., 1H), 9.62 (br. s., 1H), 7.82 (s, 1H), 7.60 (d, J = 8.1 Hz, 4H), 7.51 (d, J = 7.8 Hz, 3H), 7.35−7.44 (m, 2H), 7.26 (t, J = 7.8 Hz, 2H), 6.94−7.18 (m, 1H), 5.79 (d, J = 5.8 Hz, 1H), 3.68 (br. s., 3H), 1.56 (d, J = 5.8 Hz, 2H), 1.42−1.51 (m, 2H), 1.21−1.33 (br.m, 1H), 1.11−1.21 (m, 2H); LC/MS calcd for $C_{29}H_{26}FN_3O_4$ (m/e) 499.0; obsd, 498.0 (M − H, ES$^-$).

(*R*)-1-{4′-[1-Methyl-5-((1-(3-(trifluoromethyl)phenyl)ethoxy)-carbonylamino)-1*H*-pyrazol- 4-yl]-biphenyl-4-yl}-cyclopropanecarboxylic Acid (16). ^{1}H NMR (DMSO-d_6) δ ppm 12.34 (br. s., 1H), 9.71 (br. s., 1H), 7.45−7.85 (m, 10H), 7.39 (d, J = 8.3 Hz, 3H), 5.87 (d, J = 6.0 Hz, 1H), 3.65 (s, 3H), 1.57 (d, J = 6.0 Hz, 2H), 1.39−1.51 (m, 2H), 1.22 (br. s., 1H), 1.09−1.19 (m, 2H); LC/MS calcd for $C_{30}H_{26}F_3N_3O_4$ (m/e) 549.0; obsd, 550.1 (M + H, ES$^+$).

(*R*)-1-{4′-[5-(*sec*-Butoxycarbonylamino)-1-methyl-1*H*-pyrazol- 4-yl]-biphenyl-4-yl}-cyclopropanecarboxylic Acid (17). ^{1}H NMR (DMSO-d_6) δ ppm 12.32 (br. s., 1H), 9.38 (br. s., 1H), 7.80 (s, 1H), 7.50−7.69 (m, 6H), 7.38 (d, J = 8.3 Hz, 2H), 4.69 (br. s., 1H), 3.65 (s, 3H), 1.58 (br. s., 2H), 1.33−1.52 (m, J = 2.6 Hz, 2H), 1.22 (br. s., 3H), 1.14 (m, J = 2.6 Hz, 2H), 0.91 (br. s., 3H); LC/MS calcd for $C_{25}H_{27}N_3O_4$ (m/e) 433.0; obsd, 434.1 (M + H, ES$^+$).

(*R*)-1-{4′-[5-(1,2-Dimethyl-propoxycarbonylamino)-1-methyl-1*H*-pyrazol- 4-yl]-biphenyl-4-yl}-cyclopropanecarboxylic Acid (18). ^{1}H NMR (DMSO-d_6) δ ppm 12.34 (br. s., 1H), 9.37 (br. s., 1H), 7.81 (s, 1H), 7.49−7.68 (m, 6H), 7.38 (d, J = 8.3 Hz, 2H), 4.58 (br. s., 1H), 3.65 (s, 3H), 1.82 (br. s., 1H), 1.44 (br. s., 2H), 1.03−1.30 (m, 5H), 0.92 (br. s., 6H); LC/MS calcd for $C_{26}H_{29}N_3O_4$ (m/e) 447.0; obsd, 448.2 (M + H, ES$^+$).

1-{4′-[5-(Cyclobutoxycarbonylamino)-1-methyl-1*H*-pyrazol-4-yl]-biphenyl-4-yl}-cyclopropanecarboxylic Acid (19). ^{1}H NMR (Methanol-d$_4$) δ ppm 7.77 (s, 1H), 7.52−7.72 (m, 5H), 7.44 (d, J = 8.3 Hz, 2H), 5.01 (br. s., 1H), 3.79 (s, 3H), 2.40 (br.s., 2H), 2.05−2.29 (m, 2H), 1.78−1.94 (m, 1H), 1.46−1.76 (m, 3H), 1.12−1.42 (m, 2H); LC/MS calcd for $C_{25}H_{25}N_3O_4$ (m/e) 431.0; obsd, 432.0 (M + H, ES$^+$).

1-{4′-[1-Methyl-5-((oxetan-3-yloxy)carbonylamino)-1*H*-pyrazol- 4-yl]-biphenyl-4-yl}-cyclopropanecarboxylic Acid (20). ^{1}H NMR (DMSO-d_6) δ ppm 12.33 (br. s., 1H), 7.93 (s, 1H), 7.66−7.73 (m, J = 8.3 Hz, 2H), 7.61 (d, J = 8.3 Hz, 2H), 7.53−7.59 (m, J = 8.1 Hz, 2H), 7.42 (d, J = 8.1 Hz, 2H), 5.41 (br. s., 1H), 4.85−4.94 (m, 1H), 3.90 (t, 1H), 3.66−3.83 (m, 6H), 3.57 (br. d., 1H), 1.42−1.62 (m, 2H), 1.13−1.22 (m, 2H); LC/MS calcd for $C_{24}H_{23}N_3O_5$ (m/e) 433.0; obsd, 434.1 (M + H, ES$^+$).

1-{4′-[4-Methyl-5-((*R*)-1-phenyl-ethoxycarbonylamino)-[1,2,3]triazol-1-yl]-biphenyl-4-yl}-cyclopropanecarboxylic Acid (2). In a 350 mL reaction vial, 4-bromo-phenylboronic acid (21.17 g, 105 mmol), sodium azide (10.3 g, 158 mmol), and copper(II) acetate (1.91 g, 10.5 mmol) were combined with methanol (200 mL) to give a brown suspension. The reaction was stirred at room temperature open to the atmosphere for 23 h. The resulting mixture was concentrated, diluted with ethyl ether/hexanes, and washed with water, saturated ammonium chloride, and ammonium hydroxide solution. The organic layer was dried over $MgSO_4$ and stored in the refrigerator overnight. The crude material was warmed to room temperature, filtered, concentrated to give a red/yellow oil which was dissolved in hexanes (20 mL), and purified by flash column chromatography eluted with hexanes to obtain 1-azido-4-bromo-benzene (19.5 g, 93.4% yield) as a yellow oil. LC/MS calcd for $C_6H_4BrN_3$ (m/e) 197/199; obsd, 170/172 (M-N_2+H, ES$^+$).

In a 350 mL reaction vial, 1-azido-4-bromo-benzene (10 g, 50.5 mmol) and methyl but-2-ynoate (5.45 g, 5.56 mL, 55.5 mmol) were combined with toluene (106 mL) to give a yellow suspension. The vial was sealed and heated in an oil bath at 150 °C for 4.5 h. The mixture was cooled and stored at room temperature. The reaction was filtered, and the solid was washed with toluene and ethyl acetate (3 × 15 mL). The filtrate was concentrated, dissolved in minimal dichloromethane, and purified by flash column chromatography (0% to 50% ethyl acetate in hexanes) to give 3-(4-bromo-phenyl)-5-methyl-3*H*-[1,2,3]-triazole-4-carboxylic acid methyl ester (4.5 g, 30.1% yield) as a light brown solid. LC/MS calcd for $C_{11}H_{10}BrN_3O_2$ (m/e) 295/297; obsd, 296/298 (M + H, ES$^+$).

To a 1 L round-bottom flask containing 3-(4-bromo-phenyl)-5-methyl-3*H*-[1,2,3]triazole-4-carboxylic acid methyl ester (4.5 g, 15.2 mmol) dissolved in THF (200 mL) was added LiOH (2.77 g, 120 mmol) dissolved in water (75 mL, with heat). The solution was stirred at room temperature for 16 h. The reaction was concentrated, diluted with water, and extracted with ethyl ether. The aqueous layer was acidified with 1 N HCl, and the resulting precipitate was filtered, washed with water and hexanes, and dried over an in-house vacuum to provide 3-(4-bromo-phenyl)-5-methyl-3*H*-[1,2,3]triazole-4-carboxylic acid (4.25 g, 99% yield) as an off-white solid. LC/MS calcd for $C_{10}H_8N_3O_2$ (m/e) 281/283; obsd, 282/284 (M + H, ES$^+$).

In a 350 mL reaction vial, 3-(4-bromo-phenyl)-5-methyl-3*H*-[1,2,3]triazole-4-carboxylic acid (3.6 g, 12.8 mmol), (*R*)-1-phenyl-ethanol (3.04 g, 3 mL, 24.9 mmol), and triethylamine (3.27 g, 4.5 mL, 32.3 mmol) were combined with toluene (100 mL) to give a yellow solution. To this solution was added diphenylphosphoryl azide (8.94 g, 7 mL, 32.5 mmol). The mixture was heated in an oil bath at 65 °C for 2 h and cooled to room temperature overnight. The reaction was concentrated as a yellow viscous oil, diluted with dichloromethane, and purified by flash column chromatography (0−50% ethyl acetate in hexanes) to give [3-(4-bromo-phenyl)-5-methyl-3*H*-[1,2,3]triazol-4-yl]-carbamic acid (*R*)-1-phenyl-ethyl ester (4.07 g, 79.5% yield) as a white solid. LC/MS calcd for $C_{18}H_{17}BrN_4O_2$ (m/e) 400/402; obsd, 401/403 (M + H, ES$^+$).

In a 350 mL vial, 1-[4-(4,4,5,5-tetramethyl-[1,3,2]dioxaborolan-2-yl)-phenyl]-cyclopropanecarboxylic acid methyl ester (2.49 g, 8.22 mmol, prepared from 1-(4-bromophenyl)-cyclopropanecarboxylic acid methyl ester), [3-(4-bromo-phenyl)-5-methyl-3*H*-[1,2,3]triazol-4-yl]-carbamic acid (*R*)-1-phenyl-ethyl ester (3.0 g, 7.48 mmol), 2-dicyclohexylphosphino-2′,6′-dimethoxybiphenyl (S-Phos) (921 mg, 2.24 mmol), and palladium(II) acetate (252 mg, 1.12 mmol) were combined with toluene (120 mL) to give a light yellow solution. To this was added tripotassium phosphate (4.76 g, 22.4 mmol) dissolved in water (30.0 mL). The mixture was bubbled with nitrogen, and the vial was sealed, heated in an oil bath at 100 °C for 4 h, and cooled to room temperature overnight. The reaction was diluted with ethyl acetate (50 mL) and water (100 mL), filtered, and rinsed with water (30 mL) and ethyl acetate (50 mL). The filtrate was separated and the organic layer was dried over $MgSO_4$, filtered, concentrated, dissolved in minimal dichloromethane, and purified by flash column chromatography (0% to 50% ethyl acetate in hexanes) to give 1-{4′-[4-methyl-5-((*R*)-1-phenyl-ethoxycarbonylamino)-[1,2,3]triazol-1-yl]-biphenyl-4-yl}-cyclopropanecarboxylic acid methyl ester (2.65 g, 71.4% yield) as a white solid. LC/MS calcd for $C_{29}H_{28}N_4O_4$ (m/e) 496; obsd, 497 (M + H, ES$^+$).

{4′-[4-Methyl-5-((*R*)-1-phenyl-ethoxycarbonylamino)-[1,2,3]-triazol-1-yl]-biphenyl-4-yl}-cyclopropanecarboxylic acid methyl ester (2.65 g, 5.34 mmol) was combined with THF (50 mL) to give a yellow solution. To this was added LiOH (1.28 g, 53.4 mmol) dissolved in water (12.5 mL, heated to partially dissolve). The reaction flask was sealed and heated in an oil bath at 60 °C for 5 h. The reaction was cooled to room temperature overnight. The mixture was diluted with water (100 mL), concentrated, diluted with more water (500 mL), and acidified with 1 N HCl. The resulting precipitate was filtered, washed with water and hexanes, and dried. The crude product (2.8 g) was purified by reverse phase chromatography (C18 Silicycle 120 g, 60 mL/min, 20−100% acetonitrile/H_2O) to give 1.65 g of a white solid. This solid was crystallized from acetonitrile to provide pure compound **2** (1.48 g, 57.5% yield). LC/MS calcd for $C_{28}H_{26}N_4O_4$ (m/e) 482; obsd, 483 (M + H, ES$^+$); ^{1}H NMR (DMSO-d_6) δ 12.40 (br. s., 1H), 9.69 (br. s., 1H), 7.83 (d, J = 7.0 Hz, 2H), 7.67 (d, J = 8.3 Hz, 2H), 7.58 (d, J = 8.0 Hz, 2H), 7.47 (d, J = 8.5 Hz, 2H), 7.00−7.42 (m, 5H), 5.71 (br. s., 1H), 2.18 (s, 3H), 1.29−1.69 (m, 5H), 1.13−1.26 (m, 2H).

{4′-[4-Methyl-5-((*R*)-1-phenyl-ethoxycarbonylamino)-[1,2,3]-triazol-1-yl]-biphenyl-4-yl}-acetic Acid (21). In a 350 mL reaction vial, ethyl 2-(4-bromophenyl)acetate (25 g, 103 mmol), bis-(pinacolato)diboron (31.3 g, 123 mmol), and potassium acetate (20.2 g, 206 mmol) were combined with 1,4-dioxane (190 mL) to give a white suspension. The mixture was purged with nitrogen for 5 min, $PdCl_2$(dppf) (4.2 g, 5.74 mmol) was added, and the vial was sealed and heated in an oil bath at 80 °C for 3 h. The reaction was filtered, rinsed with ethyl ether, concentrated, diluted with water (500 mL), and extracted with ethyl ether (2 × 300 mL), and the organic layers were washed with brine (250 mL). The ethyl ether layers were combined, dried over $MgSO_4$, filtered, and concentrated as red oil. The crude material was purified by flash column chromatography (0% to 20% EtOAc in hexanes) to give [4-(4,4,5,5-tetramethyl-[1,3,2]-dioxaborolan-2-yl)-phenyl]-acetic acid ethyl ester (25.14 g, 84.2% yield) as an oil. LC/MS calcd for $C_{16}H_{23}BO_4$ (m/e) 290; obsd, 291 (M + H, ES$^+$).

In a 20 mL vial, [4-(4,4,5,5-tetramethyl-[1,3,2]dioxaborolan-2-yl)-phenyl]-acetic acid ethyl ester (79.5 mg, 0.274 mmol), [1-(4-bromo-phenyl)-5-methyl-1*H*-[1,2,3]triazol-4-yl]-carbamic acid (*R*)-1-phenyl-ethyl ester (100 mg, 0.249 mmol), tripotassium phosphate (159 mg, 0.748 mmol), 2-dicyclohexylphosphino-2′,6′-dimethoxybiphenyl (S-Phos) (30.7 mg, 0.0748 mmol), and palladium(II) acetate (8.4 mg, 0.037 mmol) were combined with toluene (2 mL) and water (0.5 mL) (previously purged with nitrogen for 20 min) to give a light yellow suspension. The mixture was bubbled with nitrogen, and the vial was sealed, heated in a dry block at 100 °C for 6 h, and cooled to room temperature overnight. The reaction was diluted with ethyl acetate (50 mL) and washed with water (50 mL) and brine. The aqueous layers were extracted with ethyl acetate (50 mL). The organic layers were combined, dried over $MgSO_4$, filtered, concentrated, dissolved in minimal dichloromethane, and purified by flash column chromatography (0% to 60% ethyl acetate in hexanes) to give {4′-[4-methyl-5-((*R*)-1-phenyl-ethoxycarbonylamino)-[1,2,3]triazol-1-yl]-biphenyl-4-yl}-acetic acid ethyl ester (40 mg, 33.1% yield) as a colorless waxy solid. LC/MS calcd for $C_{28}H_{28}N_4O_4$ (m/e) 484; obsd, 485 (M + H, ES$^+$).

In a 200 mL round-bottomed flask, {4′-[4-methyl-5-((*R*)-1-phenyl-ethoxycarbonylamino)-[1,2,3]triazol-1-yl]-biphenyl-4-yl}-acetic acid ethyl ester (34 mg, 0.0702 mmol) was combined with THF (2 mL)

to give a yellow solution. To this was dripped in LiOH (16.8 mg, 0.702 mmol) dissolved in water (0.5 mL, heated to partially dissolve). The mixture was stirred for 11 h. The reaction was diluted with water, and acidified with 1 N HCl. The resulting precipitate was filtered, washed with water and hexanes, and dried to provide compound **21** as an off-white solid. LC/MS calcd for $C_{26}H_{24}N_4O_4$ (me) 456; obsd, 457 (M + H, ES$^+$); ^{1}H NMR (DMSO-d_6) δ ppm 12.42 (br. s., 1H), 9.19−9.80 (m, 1H), 7.83 (d, J = 6.5 Hz, 2H), 7.69 (d, J = 8.0 Hz, 2H), 7.57 (d, J = 7.3 Hz, 2H), 7.08−7.47 (m, 7H), 5.69 (br. s., 1H), 3.65 (s, 2H), 2.16 (s, 3H), 1.13−1.64 (m, 3H).

Compounds **22**−**29** and **31**−**32** were prepared with the same method described for the preparation of compound **2**.

1-(4′-{5-[(*R*)-1-(2-Fluoro-phenyl)-ethoxycarbonylamino]-4-methyl-[1,2,3]triazol-1-yl}-biphenyl-4-yl)-cyclopropanecarboxylic Acid (22). ^{1}H NMR (DMSO-d_6) δ ppm 12.39 (br. s., 1H), 9.74 (br. s., 1H), 7.84 (d, J = 6.5 Hz, 2H), 7.67 (d, J = 8.0 Hz, 2H), 7.58 (d, J = 8.0 Hz, 2H), 7.47 (d, J = 8.0 Hz, 2H), 6.69−7.42 (m, 4H), 5.89 (br. s., 1H), 2.17 (br. s., 3H), 1.26−1.74 (m, 5H), 1.14−1.24 (m, 2H); LC/MS calcd for $C_{28}H_{25}FN_4O_4$ (m/e) 500; obsd, 501 (M + H, ES$^+$).

1-(4′-{4-Methyl-5-[(*R*)-1-(2-trifluoromethyl-phenyl)-ethoxycarbonylamino]-[1,2,3]triazol-1-yl}-biphenyl-4-yl)-cyclopropanecarboxylic Acid (23). ^{1}H NMR (DMSO-d_6) δ ppm 12.40 (br. s., 1H), 9.77 (br. s., 1H), 7.83 (d, J = 7.3 Hz, 2H), 7.63−7.78 (m, 5H), 7.39−7.62 (m, 5H), 5.96 (br. s., 1H), 2.15 (br. s., 3H), 1.50 (d, J = 2.3 Hz, 5H), 1.20 (d, J = 2.0 Hz, 2H); LC/MS calcd for $C_{29}H_{25}F_3N_4O_4$ (m/e) 550; obsd, 551 (M + H, ES$^+$).

1-(4′-{4-Methyl-5-[(*R*)-1-(3-trifluoromethyl-phenyl)-ethoxycarbonylamino]-[1,2,3]triazol-1-yl}-biphenyl-4-yl)-cyclopropanecarboxylic Acid (24). ^{1}H NMR (DMSO-d_6) δ ppm 12.39 (br. s., 1H), 9.47 (br. s., 1H), 7.88 (d, J = 7.8 Hz, 2H), 7.64 (dd, J = 18.7, 8.2 Hz, 4H), 7.46 (d, J = 8.3 Hz, 2H), 4.67 (br. s., 1H), 2.36 (br. s., 1H), 2.20 (s, 3H), 1.54−2.02 (m, 6H), 1.43−1.53 (m, 2H), 1.17−1.31 (m, 2H), 1.05 (br. s., 3H); LC/MS calcd for $C_{26}H_{28}N_4O_4$ (m/e) 460; obsd, 461 (M + H, ES$^+$).

1-{4′-[5-((*R*)-1,2-Dimethyl-propoxycarbonylamino)-4-methyl-[1,2,3]triazol-1-yl]-biphenyl-4-yl}-cyclopropanecarboxylic Acid (25). ^{1}H NMR (DMSO-d_6) δ ppm 12.37 (br. s., 1H), 9.43 (br. s., 1H), 7.88 (d, J = 8.0 Hz, 2H), 7.57−7.73 (m, 4H), 7.46 (d, J = 8.3 Hz, 2H), 4.50 (br. s., 1H), 2.21 (s, 3H), 1.71 (br. s., 1H), 1.40−1.57 (m, 2H), 1.00−1.32 (m, 5H), 0.84 (br. s., 6H); LC/MS calcd for $C_{25}H_{28}N_4O_4$ (m/e) 448; obsd, (M + H, ES$^+$).

1-{4′-[5-((*R*)-*sec*-Butoxycarbonylamino)-4-methyl-[1,2,3]-triazol-1-yl]-biphenyl-4-yl}-cyclopropanecarboxylic acid (26). ^{1}H NMR (DMSO-d_6) δ ppm 12.37 (br. s., 1H), 9.44 (br. s., 1H), 7.88 (d, J = 8.5 Hz, 2H), 7.56−7.72 (m, 4H), 7.46 (d, J = 8.3 Hz, 2H), 4.61 (br. s., 1H), 2.21 (s, 3H), 1.38−1.66 (m, 4H), 1.03−1.34 (m, 5H), 0.85 (dd, J = 10.7, 6.9 Hz, 3H); LC/MS calcd for $C_{24}H_{26}N_4O_4$ (m/e) 434; obsd, 435 (M + H, ES$^+$).

1-{4′-[5-(1-Cyclobutyl-ethoxycarbonylamino)-4-methyl-[1,2,3]triazol-1-yl]-biphenyl-4-yl}-cyclopropanecarboxylic Acid (27). ^{1}H NMR (DMSO-d_6) δ ppm 12.39 (br. s., 1H), 9.47 (br. s., 1H), 7.88 (d, J = 7.8 Hz, 2H), 7.64 (dd, J = 18.7, 8.2 Hz, 4H), 7.46 (d, J = 8.3 Hz, 2H), 4.67 (br. s., 1H), 2.36 (br. s., 1H), 2.20 (s, 3H), 1.54−2.02 (m, 6H), 1.43−1.53 (m, 2H), 1.17−1.31 (m, 2H), 1.05 (br. s., 3H); LC/MS calcd for $C_{26}H_{28}N_4O_4$ (m/e) 460; obsd, 461 (M + H, ES$^+$).

1-[4′-(5-*tert*-Butoxycarbonylamino-4-methyl-[1,2,3]triazol-1-yl)-biphenyl-4-yl]-cyclopropanecarboxylic Acid (28). ^{1}H NMR (DMSO-d_6) δ ppm 12.40 (br. s., 1H), 9.24 (br. s., 1H), 7.90 (d, J = 8.0 Hz, 2H), 7.58−7.71 (m, 4H), 7.46 (d, J = 8.3 Hz, 2H), 2.20 (s, 3H), 1.16−1.55 (m, 13H); LC/MS calcd for $C_{24}H_{26}N_4O_4$ (m/e) 434; obsd, 435 (M + H, ES$^+$).

{3-[4′-(1-Methanesulfonylaminocarbonyl-cyclopropyl)-biphenyl-4-yl]-5-methyl-3*H*-[1,2,3]triazol-4-yl}-carbamic Acid (*R*)-1-Phenyl-ethyl Ester (29). ^{1}H NMR (DMSO-d_6) δ ppm 11.24 (br. s., 1H), 9.68 (br. s., 1H), 7.85 (d, J = 7.0 Hz, 2H), 7.72 (d, J = 8.3 Hz, 2H), 7.59 (d, J = 7.8 Hz, 2H), 7.45 (d, J = 8.3 Hz, 2H), 7.34 (br. s., 5H), 5.70 (br. s., 1H), 3.23 (s, 3H), 2.17 (s, 3H), 1.29−1.73 (m, 5H), 1.23 (br. s., 2H); LC/MS calcd for $C_{29}H_{29}N_5O_5S$ (m/e) 559; obsd, 560 (M + H, ES$^+$).

(*R*)-1-Phenyl-ethyl-1-(4′-(1-(1*H*-tetrazol-5-yl)cyclopropyl)-biphenyl-4-yl)-4-methyl-1*H*-1,2,3-triazol-5-ylcarbamate (30). To a mixture of (*R*)-1-phenylethyl 4-methyl-1-(4-(4,4,5,5-tetramethyl-1,3,2-dioxaborolan-2-yl)phenyl)-1*H*-1,2,3-triazol-5-ylcarbamate (485 mg, 1.08 mmol), 1-(4-bromophenyl)cyclopropanecarbonitrile (360 mg, 1.62 mmol), palladium(II) acetate (36.4 mg, 0.16 mmol), 2-dicyclohexylphosphino-2′,6′-dimethoxybiphenyl (133 mg, 0.33 mmol), and potassium phosphate tribasic (689 mg, 3.25 mmol) in a vial were added toluene (9 mL) and water (2.0 mL) at room temperature under nitrogen atmosphere. The vial was sealed, and the resulting light brown suspension was heated to 105 °C and stirred for 3 h. The reaction mixture was cooled and diluted with water. The organic compound was extracted into ethyl acetate (2 × 50 mL), and the combined extracts were washed with brine solution and dried over anhydrous $MgSO_4$. Filtration and concentration gave the crude residue, which was purified by flash column chromatography eluting with 0−100% ethyl acetate in hexanes to give (*R*)-1-phenyl-ethyl-1-(4′-(1-cyanocyclopropyl)biphenyl-4-yl)-4-methyl-1*H*-1,2,3-triazol-5-yl-carbamate (190 mg, 38% yield) as a white solid. LC/MS calcd for $C_{28}H_{25}N_5O_2$ (m/e) 463; obsd, 464.8 (M + H, ES$^+$).

To a solution of (*R*)-1-phenylethyl-1-(4′-(1-cyanocyclopropyl)-biphenyl-4-yl)-4-methyl-1*H*-1,2,3-triazol-5-ylcarbamate (50 mg, 0.11 mmol) in toluene (5 mL) were added di-*n*-butyltin oxide (5.37 mg, 0.22 mmol) and azidotrimethylsilane (12.4 mg, 14.3 μL, 0.11 mmol) at room temperature under nitrogen atmosphere. The resulting cloudy solution was heated to 100 °C and stirred for 15 h. The mixture was cooled to room temperature, poured into brine solution, and extracted with ethyl acetate. The organic layer was washed with brine solution and dried over anhydrous $MgSO_4$. Filtration and concentration gave the crude product which was purified by flash column chromatography eluting with 0−100% ethyl acetate in hexanes and 10% methanol in dichloromethane to give compound **30** as a white solid (25 mg, 46% yield). LC/MS calcd for $C_{28}H_{26}N_8O_2$ (m/e) 506; obsd, 507.1 (M + H, ES$^+$); ^{1}H NMR (DMSO-d_6) δ ppm 16.08 (br. s., 1H), 9.20−9.84 (m, 1H), 7.85 (d, J = 7.0 Hz, 2H), 7.73 (d, J = 8.3 Hz, 2H), 7.52−7.65 (m, 2H), 7.46 (d, J = 8.3 Hz, 2H), 7.34 (br. s., 5H), 5.52−5.84 (m, 1H), 2.17 (s, 3H), 1.51−1.63 (m, 4H), 1.15−1.35 (m, 3H).

1-{4′-[4-Ethyl-5-((*R*)-1-phenyl-ethoxycarbonylamino)-[1,2,3]-triazol-1-yl]-biphenyl-4-yl}-cyclopropanecarboxylic Acid (31). ^{1}H NMR (DMSO-d_6) δ ppm 12.40 (br. s., 1H), 9.66 (br. s., 1H), 7.83 (d, J = 6.5 Hz, 2H), 7.67 (d, J = 8.0 Hz, 2H), 7.58 (d, J = 7.3 Hz, 2H), 7.47 (d, J = 8.0 Hz, 2H), 7.34 (br. s., 5H), 5.71 (br. s., 1H), 2.56 (d, J = 7.5 Hz, 2H), 1.36−1.60 (m, 5H), 1.16−1.23 (m, 5H); LC/MS calcd for $C_{29}H_{28}N_4O_4$ (m/e) 496; obsd, 497.1 (M + H, ES$^+$).

1-{4′-[5-((*R*)-1-Phenyl-ethoxycarbonylamino)-[1,2,3]triazol-1-yl]-biphenyl-4-yl}-cyclopropanecarboxylic Acid (32). ^{1}H NMR (DMSO-d_6) δ ppm 12.38 (br. s., 1H), 10.04 (br. s., 1H), 7.87 (d, J = 8.3 Hz, 2H), 7.82 (s, 1H), 7.68 (d, J = 8.3 Hz, 2H), 7.62 (d, J = 8.3 Hz, 2H), 7.48 (d, J = 8.0 Hz, 2H), 7.17−7.41 (m, 5H), 5.74 (d, J = 5.8 Hz, 1H), 1.34−1.62 (m, 5H), 1.21 (d, J = 2.5 Hz, 2H); LC/MS calcd for $C_{27}H_{24}N_4O_4$ (m/e) 468; obsd, 469 (M + H, ES$^+$).

1-{4′-[3-((*R*)-1-Phenyl-ethoxycarbonylamino)-[1,2,4]triazol-4-yl]-biphenyl-4-yl}-cyclopropanecarboxylic Acid (33). In a 250 mL round-bottomed flask, calcium carbonate (6.11 g, 61.0 mmol) and 4-bromoaniline (5 g, 29.1 mmol) were combined with dichloromethane (25 mL) and water (25.0 mL) to give a light brown suspension. The reaction mixture was cooled to 0 °C, and thiophosgene (3.68 g, 2.45 mL, 32.0 mmol) was added dropwise over 4 min. The reaction was stirred at 0 °C for 30 min then at 25 °C for 19 h. The reaction mixture was filtered through Celite, and the filter cake was washed with dichloromethane. The aqueous layer was back-extracted with dichloromethane (1 × 25 mL). The organic layers were combined, washed with water (1 × 25 mL) and saturated NaCl (1 × 20 mL), dried over Na_2SO_4, and concentrated *in vacuo*. The light brown solid was dried under vacuum to give 1-bromo-4-isothiocyanatobenzene (5.43 g, 87%). ^{1}H NMR (DMSO-d_6) δ ppm 7.55−7.74 (m, 2H), 7.28−7.50 (m, 2H).

In a 500 mL round-bottomed flask, 1-bromo-4-isothiocyanatobenzene (1.5 g, 7.01 mmol) was combined with 0.4 M ammonia in THF (52.5 mL, 21.0 mmol) to give a yellow solution. The reaction was

dx.doi.org/10.1021/jm301022v | *J. Med. Chem.* 2012, 55, 7920−7939

stirred at 25 °C overnight. The crude reaction mixture was concentrated *in vacuo* to afford 1-(4-bromophenyl)thiourea (1.63 g, quantitative) as a light brown solid. $(M + H)^+$ = 230.9/233.0 (*m*/*e*).

In a 250 mL round-bottomed flask, 1-(4-bromophenyl)thiourea (1.62 g, 7.01 mmol) was combined with methanol (50 mL) to give a light brown suspension. Methyl iodide (1.09 g, 482 μL, 7.71 mmol) was added, and the reaction mixture was stirred at 25 °C for 17 h. The crude reaction mixture was concentrated *in vacuo* to yield 1-(4-bromophenyl)-2-methyl-isothiourea hydroiodide (2.61 g, 100%) as a light brown powder. The material was used without further purification.

In a 250 mL round-bottomed flask, 1-(4-bromophenyl)-2-methyl-isothiourea hydroiodide (2.61 g, 7.00 mmol) was combined with water (10 mL) and ethanol (10.0 mL) to give a light brown solution. Hydrazine monohydrate (525 mg, 509 μL, 10.5 mmol) was added and the reaction was stirred at 25 °C for 20 h. The crude reaction mixture was concentrated *in vacuo* to about half volume, and silver nitrate (1.19 g, 7.00 mmol) was added with vigorous stirring. The gray/brown solid was filtered through Celite, and the filter cake was washed twice with boiling water. The filtrate was concentrated *in vacuo* to give a yellow oil. The oily material was dried under vacuum with slight heating (2.27 g). This material (2.27 g, 7.77 mmol) and formic acid (715 mg, 596 μL, 15.5 mmol) were combined to give a yellow solution. The reaction mixture was heated to 120 °C for 3.5 h. The reaction was cooled and neutralized with 3 M NaOH. The mixture was diluted with 150 mL of dichloromethane and stirred vigorously. The insoluble solid was filtered, and the phases were separated. The organic phase was dried over Na_2SO_4 and filtered. The filtered solid was combined with the dried organic phase and concentrated *in vacuo*. The residue was taken up in refluxing ethanol and filtered hot to remove a small amount of white insoluble solid. The light brown filtrate was stripped to a tan powder and dried under vacuum to afford 4-(4-bromophenyl)-4*H*-1,2,4-triazol-3-amine (1.665 g, 90%). $(M + H)^+$ = 239.0/240.9 (*m*/*e*). ^{1}H NMR (DMSO-d_6) δ ppm 8.20 (s, 1H), 7.66−7.81 (m, 2H), 7.34−7.54 (m, 2H), 5.86 (s, 2H).

In a 20 mL sealed tube, 4-(4-bromophenyl)-4*H*-1,2,4-triazol-3-amine (349 mg, 1.46 mmol), 4-(1-(methoxycarbonyl)cyclopropyl)-phenylboronic acid (450 mg, 2.04 mmol) and 2 M Na_2CO_3 (2.19 mL, 4.38 mmol) were combined with dioxane (6 mL) to give a light yellow suspension. $PdCl_2$(dppf) (95.4 mg, 117 μmol) was added, and the reaction was purged with argon. The reaction mixture was sealed and heated to 100 °C for 24 h under argon. The reaction was cooled and diluted with ethyl acetate and water. The mixture was filtered, and the filtrate was washed with water and brine. The organic layer was dried over Na_2SO_4, combined with the filtered solid, and concentrated *in vacuo*. Celite was added to the residue, and the mixture was triturated with refluxing methanol. The mixture was filtered, and the filter cake was washed twice with refluxing methanol. The filtrate was stripped *in vacuo*, and the crude material was purified by flash chromatography (0% to 10% methanol in dichloromethane) to afford methyl 1-(4′-(3-amino-4*H*-1,2,4-triazol-4-yl)biphenyl-4-yl)cyclopropanecarboxylate (257 mg, 53%) as a light brown powder. $(M + H)^+$ = 335.1 (*m*/*e*). ^{1}H NMR (DMSO-d_6) δ ppm 8.24 (s, 1H), 7.79−7.86 (m, 2H), 7.62−7.70 (m, 2H), 7.53−7.60 (m, 2H), 7.41−7.49 (m, 2H), 5.86 (s, 2H), 3.58 (s, 3H), 1.42−1.61 (m, 2H), 1.16−1.35 (m, 2H).

In a 250 mL round-bottomed flask, (*R*)-1-phenylethanol (2.01 g, 16.5 mmol) and carbonyl diimidazole (2.67 g, 16.5 mmol) were combined with ethyl acetate (40 mL) to give a colorless solution. The reaction mixture was refluxed for 20 h under argon, cooled, and diluted with ethyl acetate. The mixture was washed with water (2 × 40 mL) and saturated NaCl (1 × 20 mL), dried over Na_2SO_4, and concentrated *in vacuo*. The material crystallized upon standing to afford (*R*)-1-phenylethyl 1*H*-imidazole-1-carboxylate (3.42 g, 96%) as off white needles. ^{1}H NMR (DMSO-d_6) δ ppm 8.42 (s, 1H), 7.65 (dd, *J* = 1.8, 1.3 Hz, 1H), 7.45−7.54 (m, 2H), 7.22−7.45 (m, 3H), 7.09 (dd, *J* = 1.6, 0.9 Hz, 1H), 6.05 (q, *J* = 6.6 Hz, 1H), 1.66 (d, *J* = 6.6 Hz, 3H).

In a 250 mL round-bottomed flask, methyl 1-(4′-(3-amino-4*H*-1,2,4-triazol-4-yl)biphenyl-4-yl)cyclopropanecarboxylate (115 mg, 344 μmol) was combined with THF (6 mL) to give a light brown suspension. LiHMDS (1 M) in THF (447 μL, 447 μmol) was added, and the brown solution was stirred at 25 °C under argon for 15 min. (*R*)-1-phenylethyl 1*H*-imidazole-1-carboxylate (112 mg, 516 μmol) in 1 mL of THF was added, and the reaction mixture was stirred for 15 min at 25 °C. The reaction was quenched with water and diluted with 10% methanol in dichloromethane. Sodium sulfate was added, and the mixture was filtered through Celite, and the brown filtrate was concentrated *in vacuo*. The crude material was purified by flash column chromatography (0% to 10% methanol in dichloromethane) to afford 1-{4′-[3-((*R*)-1-phenyl-ethoxycarbonylamino)-[1,2,4]triazol-4-yl]-biphenyl-4-yl}-cyclopropanecarboxylic acid methyl ester (85 mg, 51%) as an off white solid. $(M + H)^+$ = 483.1 (*m*/*e*). ^{1}H NMR (DMSO-d_6) δ ppm 10.01 (s, 1H), 8.87 (s, 1H), 7.76−7.93 (m, 2H), 7.58−7.75 (m, 2H), 7.38−7.57 (m, 4H), 7.12−7.38 (m, 5H), 5.62 (d, *J* = 6.8 Hz, 1H), 3.58 (s, 3H), 1.47−1.60 (m, 2H), 1.34 (d, *J* = 5.6 Hz, 2H), 1.15−1.31 (m, 3H). This material (110 mg, 228 μmol) was combined with THF (5 mL) and methanol (1 mL) to give a yellow solution. LiOH (1 M) (2 mL, 2.00 mmol) was added, and the reaction was stirred at 25 °C for 17 h. The crude reaction mixture was concentrated *in vacuo*, acidified with 1 M HCl, and diluted with ethyl acetate. The organic layer was washed with water (1 × 15 mL) and saturated NaCl (1 × 15 mL), dried over Na_2SO_4 and concentrated *in vacuo*. The crude material was purified by flash column chromatography (0% to 10% methanol in dichloromethane) to afford compound **33** (86 mg, 80%) as a white solid. ^{1}H NMR (DMSO-d_6) δ ppm 12.39 (br. s., 1H), 10.01 (br. s., 1H), 8.87 (br. s., 1H), 7.81 (d, *J* = 8.3 Hz, 2H), 7.65 (d, *J* = 8.3 Hz, 2H), 7.39−7.59 (m, 4H), 7.10−7.39 (m, 5H), 5.62 (d, *J* = 6.3 Hz, 1H), 1.45−1.54 (m, 2H), 1.40 (br. s., 1H), 1.09−1.37 (m, 4H); LC/MS calcd for $C_{27}H_{24}N_4O_4$ (*m*/*e*) 468; obsd, 469 $(M + H, ES^+)$.

{4′-[1-Methyl-5-((*R*)-1-phenyl-ethoxycarbonylamino)-1*H*-[1,2,3]triazol-4-yl]-biphenyl-4-yl}-acetic Acid (34). LDA solution (2 M) in THF (20.71 mL, 41.436 mmol) was added to a stirred solution of 1-bromo-4-ethynyl-benzene (3 g, 16.57 mmol) in dry THF (40 mL) at −70 °C and stirred for 30 min. Ethyl chloroformate (11.81 mL, 74.58 mmol) was added, and the mixture was allowed to warm to ambient temperature. Stirring was continued for 2 h. The mixture was cooled and quenched with saturated NH_4Cl solution. THF was evaporated under reduced pressure, and the aqueous layer was extracted with ethyl acetate. The organic layer was dried over Na_2SO_4, concentrated, and purified by flash column chromatography using ethyl acetate and hexane as eluting solvent to give (4-bromo-phenyl)-propyonic acid ethyl ester (2.9 g, 69.13% yield) as a light yellow liquid. GC-MS $(M + H)^+$ 253 (*m*/*e*); ^{1}H NMR ($CDCl_3$) δ ppm 1.32 (t, *J* = 7.0 Hz, 3H). 4.28 (q, *J* = 7.0 Hz, 2H), 7.43 (d, *J* = 8.4 Hz, 2H), 7.51 (d, *J* = 8.4 Hz, 2H).

To a stirred solution of (4-bromo-phenyl)-propynoic acid ethyl ester (2.5 g, 9.881 mmol) in benzene (4 mL), was added trimethylsilylmethyl azide (5.108 g, 39.52 mmol). The reaction mixture was refluxed for 4 h, then cooled to rt and concentrated under reduced pressure. Crude mass was purified by normal silica gel column chromatography using ethyl acetate−hexane as eluting solvent to get two major fractions. One fraction is 5-(4-bromo-phenyl)-3-trimethylsilanylmethyl-3*H*-[1,2,3] triazole-4-carboxylic acid ethyl ester (1.7 g, 45%) as a light yellow liquid. LC-MS $(M + H)^+$ 382 (*m*/*e*); ^{1}H NMR (DMSO-d_6) δ ppm 0.10 (s, 9H), 1.21 (t, *J* = 7.2 Hz, 3H), 4.31 (m, 4H), 7.66 (s, 4H). The regio-chemistry was assigned by the ^{1}H-NOE study. The other major fraction gave 5-(4-bromo-phenyl)-1-trimethylsilanylmethyl-1*H*-[1,2,3] triazole-4-carboxylic acid ethyl ester (1.8 g, 47.7% yield) as a light yellow liquid. LC-MS $(M + H)^+$ 382 (*m*/*e*); ^{1}H NMR (DMSO-d_6) δ ppm 0.02 (s, 9H), 1.13 (t, *J* = 7.2 Hz, 3H), 3.76 (s, 2H), 4.16 (q, *J* = 7.2 Hz, 2H), 7.46 (d, *J* = 8.4 Hz, 2H), 7.74 (d, *J* = 8.4 Hz, 2H). The regio-chemistry was also assigned by the ^{1}H-NOE study.

To a stirred solution of 5-(4-bromo-phenyl)-3-trimethylsilanyl-methyl-3*H*-[1,2,3] triazole-4-carboxylic acid ethyl ester (1.9 g, 4.974 mmol) in THF (40 mL) was added water (0.18 mL, 9.948 mmol) and cooled to 0 °C. Then TBAF (1 M) solution in THF (5.9 mL, 5.9 mmol) was added, and the mixture was stirred at 0 °C for 10 min. Volatiles were distilled off, and crude mass was purified by normal silica gel column chromatography using ethyl acetate−hexane as

eluting solvent to get 5-(4-bromo-phenyl)-3-methyl-3*H*-[1,2,3] triazole-4-carboxylic acid ethyl ester (0.7 g, 45.4% yield) as an off white solid. LC-MS $(M + H)^+$ 310 (*m*/*e*); ^{1}H NMR (DMSO-d_6) δ ppm 1.23 (t, *J* = 7.0 Hz, 3H), 4.27 (s, 3H), 4.31 (q, *J* = 7.0 Hz, 2H), 7.68 (s, 4H). 5-(4-Bromo-phenyl)-3-methyl-3*H*-[1,2,3] triazole-4-carboxylic acid ethyl ester (1.2 g, 3.87 mmol) was dissolved in THF (15 mL), and lithium hydroxide solution (0.5 N, 10 mL) was added. The mixture was stirred at room temperature for 3 h. The mixture was concentrated, and the residue was dissolved in water (20 mL) and filtered. The filtrate was acidified with 2 N hydrochloric acid (3 mL). The white solid was filtered and dried to give 5-(4-bromo-phenyl)-3-methyl-3*H*-[1,2,3] triazole-4-carboxylic acid as a white solid (1.03 g, 94.4% yield). Mp 209−210 °C; LC-MS calcd for $C_{10}H_8BrN_3O_2$ (*m*/*e*) 283.0; obsd, 284.0 (M + H); ^{1}H NMR (DMSO-d_6) δ ppm 4.26 (s, 3H), 7.66−7.72 (m, 4H), 14.20 (br s, 1H).

5-(4-Bromophenyl)-3-methyl-3*H*-[1,2,3]triazole-4-carboxylic acid (500 mg, 1.77 mmol), (*R*)-1-phenylethanol (260 mg, 2.13 mmol), DPPA (537 mg, 1.95 mmol), and TEA (179 mg, 1.7 mmol) were combined in toluene (10 mL). The mixture was stirred at 90 °C for 2 h, and solvents were evaporated. The residue was extracted with ethyl acetate and water. The organic layer was washed with sodium bicarbonate solution and dried. Solvents were evaporated, and the residue was purified by flash column chromatography (ethyl acetate in hexanes 0% to 50%) to give [5-(4-bromo-phenyl)-3-methyl-3*H*-[1,2,3]triazol-4-yl]-carbamic acid (*R*)-1-phenyl-ethyl ester as an amorphous powder (440 mg, 61.9% yield). LC/MS calcd for $C_{18}H_{17}BrN_4O_2$ (*m*/*e*) 402; obsd, 402.9 (M + H); ^{1}H NMR (DMSO-d_6) δ ppm 1.55 (br, 3H), 3.83 (s, 3H), 5.76 (br s, 1H), 7.20−7.50 (m, 5H), 7.57−7.70 (m, 4H), 9.95 (br s, 1H).

[5-(4-Bromo-phenyl)-3-methyl-3*H*-[1,2,3]triazol-4-yl]-carbamic acid (*R*)-1-phenyl-ethyl ester (120 mg, 0.30 mmol), ethyl 2-(4-(4,4,5,5-tetramethyl-1,3,2-dioxaborolan-2-yl)phenyl)acetate (130 mg, 0.45 mmol), X-Phos (43 mg, 0.09 mmol), palladium acetate (10 mg, 0.045 mmol), and potassium phosphate (190 mg, 0.90 mmol) were combined in 5 mL of toluene. Deionized water (1 mL) was added, and the mixture was degassed with argon for 2 min. The mixture was sealed and stirred at 100 °C for 2 h. The mixture was extracted with ethyl acetate and water, washed with brine, and dried. Solvents were evaporated, and the residue was purified by flash column chromatography (0% to 70% ethyl acetate in hexanes) to give {4′-[1-methyl-5-((*R*)-1-phenyl-ethoxycarbonylamino)-1*H*-[1,2,3]triazol-4-yl]-biphenyl-4-yl}-acetic acid ethyl ester as an amorphous powder (70 mg, 48.3% yield). LC/MS calcd for $C_{28}H_{28}N_4O_4$ (*m*/*e*) 484.0; obsd, 485.1 (M + H); ^{1}H NMR ($CDCl_3$) δ ppm 1.31 (t, *J* = 7.2 Hz, 3H), 1.53−1.76 (m, 3H), 3.69 (s, 2H), 3.95 (s, 3H), 4.21 (q, *J* = 7.2 Hz, 2H), 5.93 (m, 1H), 6.40 (br s, 1H), 7.31−7.49 (m, 7H), 7.56−7.66 (m, 4H), 7.80 (d, J-6.8 Hz, 2H).

{4′-[1-Methyl-5-((*R*)-1-phenyl-ethoxycarbonylamino)-1*H*-[1,2,3]-triazol-4-yl]-biphenyl-4-yl}-acetic acid ethyl ester (60 mg, 0.124 mmol) was dissolved in 3 mL of THF, and lithium hydroxide solution (0.5 N, 1.0 mL) was added. The mixture was stirred at room temperature for 3 h, concentrated, and dissolved in water (8 mL). The clear solution was treated with hydrochloric acid (1 N, 0.6 mL). The mixture was filtered, and the white solid was dried to give compound **34** (51 mg, 90.2% yield). LC/MS calcd for $C_{26}H_{24}N_4O_4$ (*m*/*e*) 456.0; obsd, 457.0 (M + H); ^{1}H NMR (DMSO-d_6) δ ppm 1.12−1.32 (m, 1H), 1.59 (br, 2H), 3.64 (s, 2H), 3.89 (s, 3H), 5.80 (br m, 1H), 6.96−7.54 (m, 7H), 7.61−7.74 (m, 4H), 7.80 (d, *J* = 7.6 Hz, 2H), 9.54 and 9.95 (br s, 1H), 12.38 (br s, 1H).

1-{4′-[1-Methyl-5-((*R*)-1-phenyl-ethoxycarbonylamino)-1*H*-[1,2,3]triazol-4-yl]-biphenyl-4-yl}-cyclopropanecarboxylic Acid (35). [5-(4-Bromo-phenyl)-3-methyl-3*H*-[1,2,3]triazol-4-yl]-carbamic acid (*R*)-1-phenyl-ethyl ester (566 mg, 1.41 mmol), methyl 1-(4-(4,4,5,5-tetramethyl-1,3,2-dioxaborolan-2-yl)phenyl)-cyclopropanecarboxylate (511 mg, 1.69 mmol), X-Phos (134 mg, 0.28 mmol), palladium acetate (31.7 mg, 0.14 mmol), and potassium phosphate (898 mg, 4.23 mmol) were combined in toluene (12 mL), and degassed water (3 mL) was added. The mixture was degassed and sealed. The mixture was stirred at 95 °C for 3 h and cooled to room temperature. The mixture was extracted with ethyl acetate and water. The organic layer was washed with brine and dried. Solvents were evaporated, and the residue was purified by flash column chromatography (ethyl acetate in hexanes 10% to 70%) to give 1-{4′-[1-methyl-5-((*R*)-1-phenyl-ethoxycarbonylamino)-1*H*-[1,2,3]-triazol-4-yl]-biphenyl-4-yl}-cyclopropanecarboxylic acid methyl ester as a pale yellow solid (370 mg, 52.8% yield). LC/MS calcd for $C_{29}H_{28}N_4O_4$ (*m*/*e*) 496.0; obsd, 497.0 (M + H); ^{1}H NMR ($CDCl_3$) δ ppm 1.25 (m, 3H), 1.66 (m, 4H), 3.67 (s, 3H), 3.93 (s, 3H), 5.91 (m, 1H), 6.44 (br, 1H), 7.29−7.40 (m, 5H), 7.44 (d, *J* = 8.1 Hz, 2H), 7.57 (d, *J* = 8.3 Hz, 2H), 7.61 (d, *J* = 8.3 Hz, 2H), 7.78 (br d, *J* = 6.6 Hz, 2H). This material (50 mg) was dissolved in 1 mL of THF and 1 mL of ethanol. To this mixture was added 1 N sodium hydroxide solution (1 mL). The clear solution was stirred at room temperature for 12 h. Solvents were evaporated, and the residue was treated with 2 N hydrochloric acid (1.4 mL). The solid was filtered and rinsed with water and dried in air to give compound **35** (47.5 mg, 97.8% yield). LC/MS calcd for $C_{28}H_{26}N_4O_4$ (*m*/*e*) 482.0; obsd, 483.0 (M + H); ^{1}H NMR (DMSO-d_6) δ ppm 1.14−1.24 (m, 3H), 1.49 (m, 2H), 1.59 (m, 2H), 3.86 (s, 3H), 5.80 (m, 1H), 7.28−7.50 (m, 7H), 7.63 (d, *J* = 8.1 Hz, 2H), 7.71 (m, 2H), 7.80 (d, *J* = 7.6 Hz, 2H), 9.95 and 9.62 (br s, 1H), 12.35 (s, 1H).

Compounds **36**−**39** were prepared with the same method described in the preparation of compound **35**.

1-{3′-Fluoro-4′-[1-methyl-5-((*R*)-1- phenyl-ethoxycarbonylamino)-1*H*-[1,2,3]triazole-4-yl]-biphenyl-4-yl}-cyclopropanecarboxylic Acid (36). LC/MS calcd for $C_{28}H_{25}FN_4O_4$ (*m*/*e*) 500.0; obsd, 501.0 (M + H); ^{1}H NMR (DMSO-d_6) δ ppm 12.39 (br. s., 1H), 9.92 (br. s., 1H), 7.64−7.78 (m, 3H), 7.59 (d, *J* = 7.8 Hz, 2H), 7.37−7.50 (m, 5H), 7.02−7.37 (m, 2H), 5.74 (br. s., 1H), 3.89 (s, 3H), 1.41−1.60 (m, 4H), 1.09−1.32 (m, 3H).

1-{4′-[5-((*R*)-1,2-Dimethyl-propoxycarbonylamino)-1-methyl-1*H*-[1,2,3]triazol-4-yl]-biphenyl-4-yl}-cyclopropanecarboxylic Acid (37). ^{1}H NMR (DMSO-d_6) δ ppm 0.52 (br, 1H), 0.88 (br, 5H), 1.04−1.25 (m, 5H), 1.35−1.43 (m, 2H), 1.62−1.85 (br, 1H), 3.80 (s, 3H), 4.55 (br, 1H), 7.35 (d, *J* = 8.3 Hz, 2H), 7.57 (d, *J* = 8.3 Hz, 2H), 7.68 (d, *J* = 8.3 Hz, 2H), 7.78 (d, *J* = 8.3 Hz, 2H), 9.34 and 9.67 (br s, 1H), 12.30 (br s, 1H); LC/MS calcd for $C_{25}H_{28}N_4O_4$ (*m*/*e*) 448.0; obsd, 449.2 (M + H).

1-(4′-{1-Methyl-5-[(*R*)-1-(3-trifluoromethyl-phenyl)-ethoxycarbonylamino]-1*H*-[1,2,3]triazol-4-yl}-biphenyl-4-yl)-cyclopropanecarboxylic Acid (38). This compound was obtained from the chiral separation of the racemate by super critical fluid chromatography on Waters/Berger Multigram II using a Whelk-O1 (R,R)-column (3 × 25 cm) eluted with 50% isopropanol in CO_2 at 70 mL/min (detection at 220 nM, 100 bar backpressure, and 35 °C oven). The second fraction gave compound **38** as a white solid. LC/MS calcd for $C_{29}H_{25}F_3N_4O_4$ (*m*/*e*) 550.0; obsd, 551.0 (M + H); ^{1}H NMR (DMSO-d_6) δ ppm 1.13−1.29 (m, 3H), 1.44−1.52 (m, 2H), 1.60 (br d, 2H), 3.86 (s, 3H), 5.75−5.95 (br m, 1H), 7.43 (d, *J* = 8.1 Hz, 2.5H), 7.61 (d, *J* = 8.1 Hz, 2.5H), 7.69 (br m, 3.5H), 7.79 (d, *J* = 7.6 Hz, 3.5H), 9.65 and 10.05 (br s, 1H), 12.35 (s, 1H).

1-(4′-{1-Methyl-5-[(*S*)-1-(3-trifluoromethyl-phenyl)-ethoxycarbonylamino]-1*H*-[1,2,3]triazol-4-yl}-biphenyl-4-yl)-cyclopropanecarboxylic Acid (39). The first fraction from the chiral separation (conditions described in the preparation of **38**) gave compound **39** as a white solid.

1-{4′-[3-Methyl-5-((*R*)-1-phenyl-ethoxycarbonylamino)-3*H*-[1,2,3]triazol-4-yl]-biphenyl-4-yl}-cyclopropanecarboxylic Acid (40). This compound was prepared using the same method as that described for the preparation of compound **35**, except that 5-(4-bromo-phenyl)-1-methyl-1*H*-[1,2,3] triazole-4-carboxylic acid was used. LC/MS calcd for $C_{28}H_{26}N_4O_4$ (*m*/*e*) 482.0; obsd, 483.0 (M + H); ^{1}H NMR (DMSO-d_6) δ ppm 1.15−1.30 (m, 2H), 1.32−1.62 (m, 5H), 4.05 (s, 3H), 5.69 (br m, 1H), 7.20−7.40 (br m, 5H), 7.46 (d, *J* = 8.1 Hz, 2H), 7.59 (d, *J* = 8.1 Hz, 2H), 7.66 (d, *J* = 8.1 Hz, 2H), 7.77 (d, *J* = 7.6 Hz, 2H), 9.34 (br s, 1H), 12.39 (s, 1H).

{5-[4′-(1-Methanesulfonylaminocarbonyl-cyclopropyl)-biphenyl-4-yl]-3-methyl-3*H*-[1,2,3]triazol-4-yl}-carbamic acid (*R*)-1-phenyl-ethyl Ester (41). In a 100 mL round-bottomed flask, 1-(4-bromo-phenyl)-cyclopropanecarboxylic acid (4 g, 16.6 mmol) was combined with dichloromethane (15 mL) and 3 drops of DMF to give

a white suspension. To this was added dropwise a clear solution of oxalyl chloride (6.96 g, 4.8 mL, 54.8 mmol) dissolved in dichloromethane (6 mL). After 10 min, the mixture became clear, and the reaction was stirred at room temperature for 2 h. The reaction was concentrated, diluted with toluene and hexanes, concentrated, and stored in a freezer overnight. In a 200 mL round-bottomed flask, NaH (60% mineral dispersion, 876 mg, 36.5 mmol) was washed with hexanes, and the resulting solid was diluted with DMF (6 mL) to give a white suspension. The suspension was cooled in an ice bath, and methanesulfonamide (3.16 g, 33.2 mmol) dissolved in DMF (6 mL) was added dropwise under nitrogen. After addition (5 min), the ice bath was removed, and the reaction was warmed to room temperature overnight. The reaction was cooled in an ice bath, the acid chloride previously prepared and dissolved in DMF (6 mL) was added dropwise, and the reaction was warmed to room temperature overnight. The reaction was diluted with 0.2 N HCl (200 mL) and extracted with ethyl acetate (2 × 100 mL). The organic layers were washed with brine, combined, dried over $MgSO_4$, and concentrated. The crude material was dissolved in minimal dichloromethane and purified by flash column chromatography (0% to 60% ethyl acetate in hexanes, 0.5% acetic acid) to give *N*-[1-(4-bromo-phenyl)-cyclopropanecarbonyl]-methanesulfonamide (2.74 g, 51.9% yield) as a white solid. LC/MS calcd for $C_{11}H_{12}BrNO_3S$ (*m*/*e*) 317/319; obsd, 318/320 (M + H, ES^+). This material (2.71 g, 8.52 mmol) was combined with bis-pinacolatodiboron (3.24 g, 12.8 mmol), potassium acetate (2.51 g, 25.6 mmol), and 1,4-dioxane (63.8 mL) to give a white suspension. The mixture was purged with nitrogen for 20 min, and then $PdCl_2(dppf)CH_2Cl_2$ (701 mg, 859 μmol) was added. The vial was sealed and heated in an oil bath at 80 °C for 16 h. The reaction was diluted with ethyl acetate (150 mL), filtered, and rinsed with 0.2 M HCl (200 mL) and ethyl acetate (50 mL). The combined filtrate was mixed vigorously, filtered, and separated. The aqueous layer was extracted once with EtOAc (150 mL). The organic layers were washed with brine, combined, dried over $MgSO_4$, filtered, concentrated, and dried from dichloromethane/hexanes to give a brown solid (4 g). The crude material was supported on Celite and purified by flash column chromatography (0 to 60% EtOAc in hexanes, 0.5% AcOH) to give *N*-{1-[4-(4,4,5,5-tetramethyl-[1,3,2]dioxaborolan-2-yl)-phenyl]-cyclopropanecarbonyl}-methanesulfonamide (2.75 g, 88.4% yield) as a white solid. LC/MS calcd for $C_{17}H_{24}BNO_5S$ (*m*/*e*) 365; obsd, 366 (M + H, ES^+).

In a 20 mL vial, [5-(4-bromo-phenyl)-3-methyl-3*H*-[1,2,3]triazol-4-yl]-carbamic acid (*R*)-1-phenyl-ethyl ester (110.3 mg, 275 μmol), *N*-{1-[4-(4,4,5,5-tetramethyl-[1,3,2]dioxaborolan-2-yl)-phenyl]-cyclopropanecarbonyl}-methanesulfonamide (112 mg, 307 μmol), DPPF (38 mg, 68.5 μmol), and $PdCl_2(dppf)CH_2Cl_2$ (39 mg, 47.8 μmol) were combined with DMF (5 mL), and the mixture was bubbled with nitrogen for 20 min to give a light brown/red solution. To this was added 2 N Na_2CO_3 (550 μL, 1.1 mmol), and the red mixture had nitrogen bubbled through for 1 min. The vial was sealed, placed in a dry block, and heated at 80 °C for 4 h. The reaction was diluted with ethyl acetate (75 mL) and 0.1 M HCl (100 mL), and the layers were separated. The aqueous layer was extracted with ethyl acetate (75 mL). The organic layers were washed with brine, dried over $MgSO_4$, filtered, and concentrated to give a crude material (311 mg). The crude material was dissolved in minimal dichloromethane and purified by flash column chromatography (0% to 100% EtOAc in hexanes, 0.5% AcOH) to provide compound **41** (98.5 mg, 64% yield). LC/MS calcd for $C_{29}H_{29}N_5O_5S$ (*m*/*e*) 559; obsd, 560 (M + H, ES^+); ^1H NMR (DMSO-d_6) δ ppm 11.16 (br. s., 1H), 9.93 (br. s., 1H), 7.80 (d, *J* = 7.8 Hz, 2H), 7.62−7.76 (m, 4H), 7.06−7.57 (m, 7H), 5.65−5.93 (m, 1H), 3.85 (s, 3H), 3.20 (s, 3H), 1.38−1.76 (m, 5H), 1.20 (br. s., 2H).

{5-[4′-(1-Methanesulfonylaminocarbonyl-cyclopropyl)-biphenyl-4-yl]-3-methyl-3*H*-[1,2,3]triazol-4-yl}-carbamic Acid (*R*)-1-(3-trifluoromethyl-phenyl)-ethyl Ester (42). This compound was prepared with the same method described in the preparation of **41**. ^1H NMR (DMSO-d_6) δ ppm 11.16 (br. s., 1H), 9.47−10.15 (m, 1H), 7.53−7.94 (m, 10H), 7.41 (d, *J* = 8.3 Hz, 2H), 5.89 (br. s., 1H), 3.86 (br. s., 3H), 3.20 (s, 3H), 1.60 (br. s., 3H), 1.47−1.53 (m, 2H), 1.20 (d, *J* = 1.8 Hz, 2H); LC/MS calcd for $C_{30}H_{28}F_3N_5O_5S$ (*m*/*e*) 627; obsd, 628 (M + H, ES^+).

(4-{4-[1-Methyl-5-((*R*)-1-phenyl-ethoxycarbonylamino)-1H-[1,2,3]triazol-4-yl]-phenyl}-cyclohexyl)-acetic Acid (43). To a suspension of 5-(4-bromophenyl)-3-methyl-3*H*-[1,2,3]triazole-4-carboxylic acid (209 mg, 0.74 mmol) and sodium bicarbonate (187 mg, 2.22 mmol) in DMF (10 mL) was added an excess of benzyl bromide (380 mg, 264 μL, 2.22 mmol) at room temperature under nitrogen atmosphere. The resulting colorless reaction mixture was stirred for 15 h and then diluted with water and extracted with ethyl acetate (2 × 70 mL). The combined extracts were washed with brine solution and dried over anhydrous $MgSO_4$. Filtration and concentration gave the crude colorless oil which was purified by column chromatography eluting with ethyl acetate in hexanes (0−60%) to give 5-(4-bromophenyl)-3-methyl-3*H*-[1,2,3]triazole-4-carboxylic acid benzyl ester as a viscous oil (275 mg, 99% yield). LC/MS calcd for $C_{17}H_{14}BrN_3O_2$ (*m*/*e*) 373; obsd, 373.8 (M + H, ES^+).

To a mixture of 2-(4-hydroxycyclohexyl)acetic acid ethyl ester (3 g, 16.1 mmol), iodine (6.13 g, 24.2 mmol), imidazole (1.64 g, 24.2 mmol), and triphenylphosphine (6.34 g, 24.2 mmol) was added dichloromethane (100 mL) at room temperature under nitrogen atmosphere. The resulting brown suspension was stirred for 15 h, and the solvent was removed under vacuum. The residue was extracted with ethyl acetate, washed twice with a solution of water and methanol (3:1), and then washed with brine solution. The organic layer was dried over anhydrous $MgSO_4$, filtered, and concentrated to give the crude residue, which was purified by column chromatography eluting with ethyl acetate in hexanes (0−50%) to give 2-(4-iodocyclohexyl)-acetic acid ethyl ester (3.39 g, 71.1% yield) as a viscous light yellow oil. ^1H NMR of this product indicated that it contained ∼30−40% of elimination product (olefin), which was not separable on TLC.

To a 3-neck 50 mL round-bottom flask, equipped with an additional funnel and thermometer, was added zinc dust (490 mg, 7.5 mmol) at room temperature under nitrogen atmosphere. THF (2 mL) was added to cover the zinc dust followed by the addition of 1,2-dibromoethane (60.6 mg, 27.8 μL, 0.322 mmol). The mixture was heated with a heat gun until evolution of ethylene gas ceased. The suspension was cooled to room temperature, chlorotrimethylsilane (35.0 mg, 40.8 μL, 0.322 mmol) was added, and the mixture was stirred for 15 min at room temperature. Then, a solution of 2-(4-iodocyclohexyl)acetic acid ethyl ester (740 mg, 2.5 mmol) in THF (2 and 1 mL for rinsing) was added dropwise for 5 min. After addition, the reaction mixture was heated to 60 °C in an oil bath, and stirred for 3 h. The excess zinc dust was allowed to settle (15 h) to give a colorless solution. In another 2-neck 25 mL round-bottom flask, palladium(II) acetate (18.1 mg, 0.081 mmol) and 2-dicyclohexylphosphino-2′,6′-dimethoxybiphenyl (66.2 mg, 0.162 mmol) were charged, and the flask was purged with nitrogen gas. Then, THF (1 mL) was added, and the resulting light brown suspension was stirred for 5 min before the addition of a solution of 5-(4-bromophenyl)-3-methyl-3*H*-[1,2,3]triazole-4-carboxylic acid benzyl ester (120 mg, 0.322 mmol) in THF (3 mL) at room temperature under nitrogen atmosphere. The above prepared colorless zinc solution was added to this mixture. The mixture was heated to 60 °C and stirred for 5 h. The reaction was cooled to room temperature and diluted with saturated ammonium chloride solution and ethyl acetate. The organic extracts were washed with brine and dried over anhydrous $MgSO_4$. Filtration and evaporation of solvents gave a crude light yellow residue, which was purified by column chromatography eluting with ethyl acetate in hexanes (0−100%) to provide 5-[4-(4-ethoxycarbonylmethyl-cyclohexyl)-phenyl]-3-methyl-3*H*-[1,2,3]triazole-4-carboxylic acid benzyl ester (55 mg, 37.0% yield) as a light brown oil. LC/MS calcd for $C_{27}H_{31}N_3O_4$ (*m*/*e*) 461; obsd, 462.1 (M + H, ES^+). This material (51 mg, 0.11 mmol) and 10% Pd/C (58.8 mg, 0.552 mmol) were combined with ethyl acetate (5 mL) at room temperature and hydrogenated with a hydrogen balloon overnight. The reaction mixture was filtered, and the charcoal was washed with hot ethyl acetate (50 mL), THF (25 mL), CH_3CN (75 mL), and ethanol (25 mL). The filtrate was concentrated, and the residue was dried under high vacuum to obtain 5-[4-(4-ethoxycarbonylmethyl-cyclohexyl)-

phenyl]-3-methyl-3*H*-[1,2,3]triazole-4-carboxylic acid (40 mg, 97.5% yield) as a white solid. LC/MS calcd for $C_{20}H_{25}N_3O_4$ (*m*/*e*) 371; obsd, 372.3 (M + H, ES$^+$). This material was converted to the desired carbamate followed by saponification (2 steps) to afford compound **43**. ^{1}H NMR (DMSO-d_6) δ ppm 12.04 (br. s., 1H), 9.85 (br. s., 1H), 7.62 (d, J = 7.3 Hz, 2H), 6.84−7.54 (m, 7H), 5.78 (br. s., 1H), 3.83 (s, 3H), 2.16 (d, J = 6.8 Hz, 2H), 1.65−1.93 (m, 5H), 1.39−1.64 (m, 5H), 1.01−1.35 (m, 3H). LC/MS calcd for $C_{26}H_{30}N_4O_4$ (*m*/*e*) 462; obsd, 463.3 (M + H, ES$^+$).

Calculations of Torsion Angle Preferences. Truncated models of compounds **32**, **33**, and **2** were built using Maestro version 9.1 (Schrodinger, LLC, New York, NY). Specifically, the biaryl substitutions linked to the triazole were truncated to contain only a single phenyl group. All potential energies were calculated using Jaguar (Schrodinger, LLC, New York, NY) using the Density Functional Theory (DFT) method with the B3LYP hybrid functional and the 6-31G** basis set. The torsion angle was defined using the atom at the 4-position (in **32** and **2**) or the 2-position (in **33**) of the triazole, the carbon of the triazole bonded to the carbamate, the nitrogen of the carbamate, and the carbonyl carbon of the carbamate. The triazole-carbamate torsion angle was scanned in 20° increments, with up to 50 rounds of geometry optimization of the remaining degrees of freedom at each torsion angle.

LPA1/3 Calcium Flux Assay Using a Fluorometric Imaging Plate Reader (FLIPR Assay). The ChemiScreen Calcium-optimized stable cell lines containing the human recombinant LPA1 or LPA3 Lysophospholipid receptors along with the parental line were purchased from Chemicon International, Inc./Millipore. One day prior to assay, cells were harvested and seeded at 10,000 cells per well into 384 well black/clear tissue culture treated plates. On the day of the assay, a calcium loading dye (Calcium-4, Molecular Devices) in Hank's Balanced Salt Solution containing 20 mM HEPES and 2.5 mM probenecid was added to each well, and plates were then incubated for 30 min at 37 °C. After incubation, 20 μL of test compound in assay buffer with 2.2% DMSO was transferred to the cell plate by the FLIPR. Compound addition was monitored by the FLIPR to detect any agonist activity of the compounds. Plates were then incubated for 30 min at room temperature protected from light. After incubation, plates were returned to the FLIPR, and 20 μL of 4.5 μM LPA (18:1) or ionomycin (for parental line) was added to the cell plates. The fluorescence was continuously monitored before, during, and after sample addition for a total elapsed time of 100 s. Responses (increase in peak fluorescence) in each well following agonist addition is determined. The initial fluorescence reading from each well, prior to ligand stimulation, was used as zero baseline value for the data from that well. The responses are expressed as % inhibition of the buffer control. The IC_{50} value, defined as the concentration of a compound that is required for 50% inhibition of the buffer control, was calculated by fitting the percent inhibition data for 10 concentrations to a sigmoidal dose−response (4 parameter logistic) model using the Genedata Condoseo program [model 205, $F(x) = (A + (B - A)/(1+((C/x)^D)))$].

Cell Culture of NHLFs. NHLFs obtained from healthy, nonsmoking donors, (Lonza Rockland Inc., Rockland, ME, USA) were grown at 37 °C in a humidified 5% CO_2 atmosphere in complete medium (FGM fibroblast basal medium supplemented with 0.5 mL of recombinant human fibroblast growth factor-B, 0.5 mL of insulin, 0.5 mL of gentamicin sulfate amphotericin-B, and 2% (v/v) fetal bovine serum (FBS) according to the manufacturer's instructions). Where indicated, NHLFs were serum-starved in basal medium (FGM fibroblast basal medium supplemented with 0.5 mL of recombinant human fibroblast growth factor-B, 0.5 mL of insulin, 0.5 mL of gentamicin sulfate amphotericin-B, 0.1% (v/v) FBS, and 0.1% (v/v) fatty acid-free BSA). For all experiments, NHLFs were used between passages 5 and 9.

Assessment of Proliferation Using BrdU Incorporation. NHLFs were seeded in BioCoat Collagen I 96-well clear black plates (BD Biosciences, Franklin Lakes, NJ, USA) at a density of 5 × 10^3 cells/well and incubated overnight in complete medium after which the cells were starved with basal media containing 0.1% (v/v) FBS and 0.1% (v/v) fatty acid-free BSA for 24 h. The cells were incubated with vehicle or LPAR antagonists for 1 h at the concentrations indicated and were then stimulated with LPA (18:1) at the indicated concentration for 48 h. Proliferation was assessed by determining the incorporation of BrdU using a BrdU proliferation assay kit (Calbiochem, San Diego, CA, USA) in accordance with the manufacturer's protocol. The degree of BrdU incorporation was assessed using an EnVision Multilabel Reader (Perkin-Elmer Inc., San Jose, CA, USA).

Three-Dimensional Collagen Gel Contraction Assay. Lung fibroblast contraction was assessed using a commercially available three-dimensional collagen gel contraction kit (Cell Biolabs, San Diego, CA, USA) and performed according to the manufacturer's instructions. Briefly, NHLFs (2.5 × 10^5 cells/well) were mixed 1:4 with a collagen gel lattice mixture using the volumes indicated in the manufacturer's instructions and 0.5 mL plated per well in a 24-well plate, which was incubated for 2 h at 37 °C to allow gel polymerization. Following gel polymerization, 1 mL of basal media containing 0.1% (v/v) FBS, 0.1% (v/v) fatty acid-free BSA, and either vehicle or LPAR antagonists was added to each well. The gels were detached, and then vehicle or LPA (18:1) at the concentrations indicated was added. Then, 18 h later the images of the contracted gel discs were obtained and quantitation performed by assessing the weight of the gel discs.

LPA-Induced Histamine Release in Mice. Male C57BL6/J mice (7−9 weeks old) were purchased from the Jackson Laboratory (Bar Harbor, ME) and housed under pathogen-free conditions with food and water *ad libitum*. All animal care and experimental procedures were approved by the Roche Animal Care and Use Committee, which is a facility accredited by the American Association for the Accreditation of Laboratory Animal Care (AAALAC).

For dose−response studies, mice received intravenous LPA challenge (0−1000 μg/mouse in 0.1% fatty acid-free bovine serum albumin) and then were sacrificed 3 min after LPA administration with 4% isoflurane. Blood was collected into EDTA-coated tubes, centrifuged 10,000*g* for 10 min at 4 °C, and frozen on dry ice. The plasma was stored at −80 °C before analysis. Histamine concentrations were measured by ELISA (Oxford Biomedical Research) based on the manufacturer's instructions. Data are presented as the mean ± SEM of n = 5−6 mice.

For the compound efficacy studies, mice received compound **2** (1−100 mg/kg), the LPA1R antagonist AM095 (100 mg/kg) as a positive control, or vehicle per os (p.o.) 2 h prior to the intravenous administration of LPA (100 μg/mouse). Histamine levels in the plasma were determined as described above. The plasma concentrations of compound **2** were analyzed by liquid chromatography/mass spectrometry. Data are expressed as the mean ± SEM of n = 5−8 mice. Significance (relative to the LPA vehicle control) was determined using a one-way ANOVA and Dunnet's posthoc test. The relationship between plasma histamine and compound **2** concentrations was determined using a Spearman's rank correlation coefficient.

AUTHOR INFORMATION

Corresponding Author

*Phone: (973)235-3240. E-mail: yimin.qian@roche.com.

Notes

The authors declare no competing financial interest.

ACKNOWLEDGMENTS

We thank Paul Gillespie, Karen Lackey, and Satwant Narula for constructive discussion, Ted Lambros for SFC chiral separation, and Gino Sasso for the ^{1}H NMR NOE study.

ABBREVIATIONS USED

LPA, lysophosphatidic acid; LPAR, lysophosphatidic acid receptor; LPA1, lysophosphatidic acid receptor-1; IPF, idiopathic pulmonary fibrosis; ECM, extracellular matrix; BALF, bronchoalveolar lavage fluid; UUO, unilateral ureteral

obstruction; NHLF, normal human lung fibroblast; BrdU, bromodeoxyuridine; FLIPR, fluorometric imaging plate reader

REFERENCES

(1) Datta, A.; Scotton, C. J.; Chambers, R. C. Novel therapeutic approaches for pulmonary fibrosis. *Br. J. Pharmacol.* **2011**, *163* (1), 141−172.

(2) Scotton, C. J.; Chambers, R. C. Molecular targets in pulmonary fibrosis: the myofibroblast in focus. *Chest* **2007**, *132* (4), 1311−1321.

(3) Parrill, A. L.; Baker, D. L. Autotaxin inhibitors: a perspective on initial medicinal chemistry efforts. *Expert Opin. Ther. Pat.* **2010**, *20* (12), 1619−1625.

(4) Lin, M. E.; Herr, D. R.; Chun, J. Lysophosphatidic acid (LPA) receptors: signaling properties and disease relevance. *Prostaglandins Other Lipid Mediators* **2010**, *91* (3−4), 130−138.

(5) Choi, J. W.; Herr, D. R.; Noguchi, K.; Yung, Y. C.; Lee, C. W.; Mutoh, T.; Lin, M. E.; Teo, S. T.; Park, K. E.; Mosley, A. N.; Chun, J. LPA receptors: subtypes and biological actions. *Annu. Rev. Pharmacol. Toxicol.* **2010**, *50*, 157−186.

(6) Mutoh, T.; Rivera, R.; Chun, J. Insights into the pharmacological relevance of lysophospholipid receptors. *Br. J. Pharmacol.* **2012**, *165* (4), 829−844.

(7) Shiomi, T.; Boudreault, F.; Padem, N.; Higashiyama, S.; Drazen, J. M.; Tschumperlin, D. J. Lysophosphatidic acid stimulates epidermal growth factor-family ectodomain shedding and paracrine signaling from human lung fibroblasts. *Wound Repair Regener.* **2011**, *19* (2), 229−240.

(8) Yin, Z.; Watsky, M. A. Chloride channel activity in human lung fibroblasts and myofibroblasts. *Am. J. Physiol. Lung Cell Mol. Physiol.* **2005**, *288* (6), L1110−1116.

(9) Mio, T.; Liu, X.; Toews, M. L.; Rennard, S. I. Lysophosphatidic acid augments fibroblast-mediated contraction of released collagen gels. *J. Lab. Clin. Med.* **2002**, *139* (1), 20−27.

(10) Pradere, J. P.; Klein, J.; Gres, S.; Guigne, C.; Neau, E.; Valet, P.; Calise, D.; Chun, J.; Bascands, J. L.; Saulnier-Blache, J. S.; Schanstra, J. P. LPA1 receptor activation promotes renal interstitial fibrosis. *J. Am. Soc. Nephrol.* **2007**, *18* (12), 3110−3118.

(11) Tager, A. M.; LaCamera, P.; Shea, B. S.; Campanella, G. S.; Selman, M.; Zhao, Z.; Polosukhin, V.; Wain, J.; Karimi-Shah, B. A.; Kim, N. D.; Hart, W. K.; Pardo, A.; Blackwell, T. S.; Xu, Y.; Chun, J.; Luster, A. D. The lysophosphatidic acid receptor LPA1 links pulmonary fibrosis to lung injury by mediating fibroblast recruitment and vascular leak. *Nat. Med.* **2008**, *14* (1), 45−54.

(12) Xue, J.; Gan, L.; Li, X.; Li, J.; Qi, G.; Wu, Y.; Fu, X.; Mao, Q.; Ao, R.; Lang, J.; Lu, Y. Effects of lysophosphatidic acid and its receptors LPA(1/3) on radiation pneumonitis. *Oncol. Rep.* **2010**, *24* (6), 1515−1520.

(13) Rancoule, C.; Pradere, J. P.; Gonzalez, J.; Klein, J.; Valet, P.; Bascands, J. L.; Schanstra, J. P.; Saulnier-Blache, J. S. Lysophosphatidic acid-1-receptor targeting agents for fibrosis. *Expert Opin. Invest. Drugs* **2011**, *20* (5), 657−667.

(14) Fells, J. I.; Tsukahara, R.; Liu, J.; Tigyi, G.; Parrill, A. L. Structure-based drug design identifies novel LPA3 antagonists. *Bioorg. Med. Chem.* **2009**, *17* (21), 7457−7464.

(15) Heasley, B. H.; Jarosz, R.; Lynch, K. R.; Macdonald, T. L. Initial structure-activity relationships of lysophosphatidic acid receptor antagonists: discovery of a high-affinity LPA1/LPA3 receptor antagonist. *Bioorg. Med. Chem. Lett.* **2004**, *14* (11), 2735−2740.

(16) East, J. E.; Carter, K. M.; Kennedy, P. C.; Schulte, N. A.; Toews, M. L.; Lynch, K. R.; Macdonald, T. L. Development of a phosphatase-resistant, L-tyrosine derived LPA1/LPA3 dual antagonist. *MedChemComm* **2011**, *2* (4), 325−330.

(17) Ohta, H.; Sato, K.; Murata, N.; Damirin, A.; Malchinkhuu, E.; Kon, J.; Kimura, T.; Tobo, M.; Yamazaki, Y.; Watanabe, T.; Yagi, M.; Sato, M.; Suzuki, R.; Murooka, H.; Sakai, T.; Nishitoba, T.; Im, D. S.; Nochi, H.; Tamoto, K.; Tomura, H.; Okajima, F. Ki16425, a subtype-selective antagonist for EDG-family lysophosphatidic acid receptors. *Mol. Pharmacol.* **2003**, *64* (4), 994−1005.

(18) Swaney, J. S.; Chapman, C.; Correa, L. D.; Stebbins, K. J.; Bundey, R. A.; Prodanovich, P. C.; Fagan, P.; Baccei, C. S.; Santini, A. M.; Hutchinson, J. H.; Seiders, T. J.; Parr, T. A.; Prasit, P.; Evans, J. F.; Lorrain, D. S. A novel, orally active LPA(1) receptor antagonist inhibits lung fibrosis in the mouse bleomycin model. *Br. J. Pharmacol.* **2010**, *160* (7), 1699−1713.

(19) Swaney, J. S.; Chapman, C.; Correa, L. D.; Stebbins, K. J.; Broadhead, A. R.; Bain, G.; Santini, A. M.; Darlington, J.; King, C. D.; Baccei, C. S.; Lee, C.; Parr, T. A.; Roppe, J. R.; Seiders, T. J.; Ziff, J.; Prasit, P.; Hutchinson, J. H.; Evans, J. F.; Lorrain, D. S. Pharmacokinetic and pharmacodynamic characterization of an oral lysophosphatidic acid type 1 receptor-selective antagonist. *J. Pharmacol. Exp. Ther.* **2011**, *336* (3), 693−700.

(20) Castelino, F. V.; Seiders, J.; Bain, G.; Brooks, S. F.; King, C. D.; Swaney, J. S.; Lorrain, D. S.; Chun, J.; Luster, A. D.; Tager, A. M. Amelioration of dermal fibrosis by genetic deletion or pharmacologic antagonism of lysophosphatidic acid receptor 1 in a mouse model of scleroderma. *Arthritis Rheum.* **2011**, *63* (5), 1405−1415.

(21) Xu, M. Y.; Porte, J.; Knox, A. J.; Weinreb, P. H.; Maher, T. M.; Violette, S. M.; McAnulty, R. J.; Sheppard, D.; Jenkins, G. Lysophosphatidic acid induces alphavbeta6 integrin-mediated TGF-beta activation via the LPA2 receptor and the small G protein G alpha(q). *Am. J. Pathol.* **2009**, *174* (4), 1264−1279.

(22) Beck, H. P.; Kohn, T.; Rubenstein, S.; Hedberg, C.; Schwandner, R.; Hasslinger, K.; Dai, K.; Li, C.; Liang, L.; Wesche, H.; Frank, B.; An, S.; Wickramasinghe, D.; Jaen, J.; Medina, J.; Hungate, R.; Shen, W. Discovery of potent LPA2 (EDG4) antagonists as potential anticancer agents. *Bioorg. Med. Chem. Lett.* **2008**, *18* (3), 1037−1041.

(23) Lukyanov, S. M.; Bliznets, I. V.; Shorshnev, S. V.; Aleksandrov, G. G.; Stepanov, A. E.; Vasil'ev, A. A. Microve-assisted synthesis and transformations of sterically hindered 3-(5-tetrazolyl)pyridines. *Tetrahedron* **2006**, *62*, 1849−1863.

(24) Meanwell, N. A. Synopsis of some recent tactical application of bioisosteres in drug design. *J. Med. Chem.* **2011**, *54* (8), 2529−2591.

(25) Sardar, V. M.; Bautista, D. L.; Fischer, D. J.; Yokoyama, K.; Nusser, N.; Virag, T.; Wang, D. A.; Baker, D. L.; Tigyi, G.; Parrill, A. L. Molecular basis for lysophosphatidic acid receptor antagonist selectivity. *Biochim. Biophys. Acta* **2002**, *1582* (1−3), 309−317.

(26) Pierce, A. C.; ter Haar, E.; Binch, H. M.; Kay, D. P.; Patel, S. R.; Li, P. CH-O and CH-N hydrogen bonds in ligand design: a novel quinazolin-4-ylthiazol-2-ylamine protein kinase inhibitors. *J. Med. Chem.* **2005**, *48*, 1278−1281.

(27) Hayashi, M.; Okabe, K.; Kato, K.; Okumura, M.; Fukui, R.; Fukushima, N.; Tsujiuchi, T. Differential function of lysophosphatidic acid receptors in cell proliferation and migration of neuroblastoma cells. *Cancer Lett.* **2012**, *316* (1), 91−96.

(28) Ramirez, G.; Hagood, J. S.; Sanders, Y.; Ramirez, R.; Becerril, C.; Segura, L.; Barrera, L.; Selman, M.; Pardo, A. Absence of Thy-1 results in TGF-beta induced MMP-9 expression and confers a profibrotic phenotype to human lung fibroblasts. *Lab. Invest.* **2011**, *91* (8), 1206−1218.

(29) Funke, M.; Zhao, Z.; Xu, Y.; Chun, J.; Tager, A. M. The lysophosphatidic acid receptor LPA1 promotes epithelial cell apoptosis after lung injury. *Am. J. Respir. Cell Mol. Biol.* **2012**, *46* (3), 355−364.

(30) Yamamoto, T.; Fujita, K.; Asari, S.; Chiba, A.; Kataba, Y.; Ohsumi, K.; Ohmuta, N.; Iida, Y.; Ijichi, C.; Iwayama, S.; Fukuchi, N.; Shoji, M. Synthesis and evaluation of isoxazole derivatives as lysophosphatidic acid (LPA) antagonists. *Bioorg. Med. Chem. Lett.* **2007**, *17* (13), 3736−3740.

(31) Hutchinson J. H.; Seiders T. J.; Wang B. Compounds as Lysophosphatidic Acid Receptor Antagonists. Patent application WO2011/017350. (b) Hutchinson J. H.; DeArmond I. M.; Seiders T. J. Lysophosphatidic Acid Receptor Antagonist for the Treatment of Dermal Conditions. Patent application WO2011/159635. (c) Brittain J. E.; Seiders T. J.; Hutchinson, J. H.; King C. D.; Rosso, V. W. Patent application WO2012/078805.